Testing gravity theories with cosmic microwave background in the degenerate higher-order scalar-tensor theory

Takashi Hiramatsu[1,*] and Daisuke Yamauchi[2,†]

[1]Department of Physics, Rikkyo University, Toshima, Tokyo 171-8501, Japan
[2]Faculty of Engineering, Kanagawa University, Kanagawa 221-8686, Japan

(Received 28 April 2020; accepted 10 September 2020; published 19 October 2020)

We study the cosmic microwave background (CMB) in the framework of the degenerate higher-order scalar-tensor (DHOST) theory to test gravity theories. This theoretical framework includes the wide class of dark energy models such as the Horndeski theory and its extensions as certain limits, and the general relativity can be also recovered. In this study, to test gravity theories with CMB, we formulate the linear perturbations of gravity and matter in the theory and their effective description parametrized by time-dependent effective field theory (EFT) parameters, α_i ($i = B, K, T, M, H, L$) and β_i ($i = 1, 2, 3$). Based on the resultant DHOST framework, we develop a numerical code to solve Boltzmann equations consistently. We then show that the angular power spectra of the CMB temperature anisotropies, E-mode, and lensing potential as a demonstration and find that the parameter characterizing the DHOST theory, β_1, provides the larger modifications of the spectra, compared with other EFT parameters. We also show the results in the case of a specific model in which the cosmic expansion and the EFT parameters are consistently determined.

DOI: 10.1103/PhysRevD.102.083525

I. INTRODUCTION

The nearly simultaneous detection of the gravitational event GW170817 and its optical counterpart GRB170817A has put a strong constraint on the speed of gravitational waves propagating from a neutron star binary such that it should not deviate from that of light, $|c_{\rm gw} - c| \leq 10^{-15}$ [1–3], which forbids any extensions of general relativity (GR) predicting a large deviation of $c_{\rm gw}$. This measurement can therefore put constraints on scalar-tensor theory as alternative to dark energy [4–8]. To explore the theories of gravity beyond GR, the degenerate higher-order scalar-tensor (DHOST) theory [9,10] (see [11] for review and references therein) is useful since most of known theories of gravity so far, such as the Horndeski theory [12–14] and the beyond-Horndeski theory [15,16], are included. The DHOST theory has eight arbitrary functions of the scalar field ϕ and $X = \partial_\mu\phi\partial^\mu\phi$, dubbed as $P(\phi, X), Q(\phi, X)$, $f_2(\phi, X)$, and $a_i(\phi, X)$ with $i = 1, \ldots, 5$. There are three degeneracy conditions eliminating the unwanted higher-order time-derivative terms. The measurement of GW170817 strongly implies that the propagation speed of gravitational waves and the speed of light strictly coincide, that is, $c_{\rm gw} = c$. Even when imposing this condition, a certain subclass of type-I quadratic DHOST theory survived [7,8]. This theory is still phenomenologically interesting because the Vainshtein screening mechanism is successfully implemented outside matter, whereas its partial breaking occurs inside [8,17–20]. This phenomenon can be used to put the additional constraints on the DHOST theory. Moreover, several theoretical constraints on the DHOST theory have been discussed in the literatures [21,22].

However, the propagation of gravitational waves from GW170817 as well as the local measurement of gravity can put any constraints on gravity theories at the relatively low redshift, $z \lesssim 0.01$. In this sense, there is still a large viability of extended gravity theories whose deviation from GR emerges at high redshift, say, $z \gtrsim 1$. One of the well-established experiments at such a high redshift is the cosmic microwave background (CMB). As of the Planck experiments, we know that the Λ-Cold Dark Matter (ΛCDM) model can well describe our Universe [23]. Hence, the extended gravity theories are required to satisfy that the background evolution should be almost the same as ΛCDM. We then need to explore the dynamics of linear perturbations of gravity and matter contents in the extended theories of gravity with keeping the background the fiducial one.

In this paper, we investigate the time evolutions of the metric perturbations, density/velocity perturbations of fluid components, and the perturbation of the scalar field after reheating. To do so, we employ the effective description of the DHOST theory, following the approach called the effective field theory (EFT) of dark energy [24–32]. The EFT describing the DHOST theory has nine

*hiramatz@rikkyo.ac.jp
†yamauchi@jindai.jp

time-dependent parameters, and the degeneracy conditions mentioned later reduce them to six parameters, $\alpha_i(t)$ with $i = K, B, T, M, H$ and $\beta_1(t)$, which are defined as the coefficients of terms such as $\delta K^{ij}\delta K_{ij}$ and $\delta K \delta R$ in the ADM Lagrangian and vanish in GR. The EFT parameters are frequently assumed to scale as (e.g., [26])

$$\alpha_i(t) = \alpha_{i,0}\frac{\Omega_{\rm DE}(t)}{\Omega_{\rm DE,0}}, \qquad \beta_1(t) = \beta_{1,0}\frac{\Omega_{\rm DE}(t)}{\Omega_{\rm DE,0}}, \quad (1)$$

where $\Omega_{\rm DE}(t)$ and $\Omega_{\rm DE,0}$ denote the fractional energy density of the dark energy and its present value. Following this parametrization, the EFT parameters are negligible in the early Universe where $\Omega_{\rm DE}(t)$ is quite small, recovering GR. Therefore, we do not need to consider the modification of the initial perturbations in solving the Boltzmann equation from very high redshift. Then we compute the angular power spectra of the CMB temperature anisotropies (C_ℓ^{TT}), E-mode polarization (C_ℓ^{EE}), and the lensing potential ($C_\ell^{\phi\phi}$).

The EFT approach is useful to for us to know the impacts of modification of each term in the Lagrangian on the time evolution of the perturbations in the fixed background. Strictly speaking, however, the background geometry is not consistently treated in the EFT approach. In the DHOST theory, the time evolution of background scalar field $\dot{\phi}_0(t)$ modifies the Friedmann equation and determines how the EFT parameters evolve in time. To demonstrate a consistent way to describe both the background and the perturbations, we also solve the set of equations with the EFT parameters and the cosmic expansion history computed from the DHOST theory with the parametrization of the arbitrary functions therein proposed by Crisostomi and Koyama [33].

This paper is organized as follows. In Sec. II, we derive the evolution equations of the background and linear perturbations in the DHOST theory. In Sec. III, we derive them in the effective description of the type-I DHOST theory and explicitly show the relations between the EFT parameters, α_i and β_1, and the scalar field. In Sec. IV, we briefly explain the setup for the numerical calculations. In Sec. V, we show the angular power spectra and how precisely we can estimate the EFT parameters according to the Fisher analysis. In Sec. VI, we demonstrate a consistent treatment of the background geometry and the perturbations with a specific model. Finally, we conclude in Sec. VII. Since the derived equations are too long to show in the main text, the Appendixes supplement the main text. Throughout the paper, we use the unit with $c = \hbar = 1$, and $M_{\rm pl}^{-2} \coloneqq 8\pi G$ where G is the usual Newton constant.

II. DHOST THEORY

A. Basics

We consider the quadratic DHOST theory, whose action is given as [9]

$$S = \int d^4x\sqrt{-g}\mathcal{L}_{\rm DHOST} + \int d^4x\sqrt{-g}\mathcal{L}_m, \quad (2)$$

where we assume that the Lagrangian for matter, $\mathcal{L}_m$, minimally couples to gravity, and

$$\mathcal{L}_{\rm DHOST} \coloneqq P(\phi,X) + Q(\phi,X)\Box\phi + f_2(\phi,X)^{(4)}R + \sum_{i=1}^{5} a_i(\phi,X)\mathcal{L}_i, \quad (3)$$

with P, Q, f_2, and a_i being arbitrary functions of ϕ and $X \coloneqq \partial_\mu\phi\partial^\mu\phi$. The Lagrangians for derivative couplings of the scalar field are described as

$$\mathcal{L}_1 \coloneqq \phi_{\mu\nu}\phi^{\mu\nu}, \qquad \mathcal{L}_2 \coloneqq (\Box\phi)^2, \qquad \mathcal{L}_3 \coloneqq (\Box\phi)\phi^\mu\phi_{\mu\nu}\phi^\nu,$$
$$\mathcal{L}_4 \coloneqq \phi^\mu\phi_{\mu\rho}\phi^{\rho\nu}\phi_\nu, \qquad \mathcal{L}_5 \coloneqq (\phi^\mu\phi_{\mu\nu}\phi^\nu)^2, \quad (4)$$

with $\phi_\mu \coloneqq \nabla_\mu\phi$ and $\phi_{\mu\nu} \coloneqq \nabla_\mu\nabla_\nu\phi$. In this paper, we consider the type-I degeneracy condition to avoid the ghost instability, which is given by the following three conditions [9]:

$$\begin{aligned} a_2 &= -a_1, \\ a_4 &= \frac{1}{8(f_2 + a_2X)^2}[16Xa_2^2 + 4(3f + 16Xf_X)a_2^2 + (16X^2f_X - 12Xf)a_3a_2 - X^2fa_3^2 \\ &\quad + 16f_X(3f + 4Xf_X)a_2 + 8f(Xf_X - f)a_3 + 48ff_X^2], \\ a_5 &= \frac{(4f_X + 2a_2 + Xa_3)(-2a_2^2 + 3Xa_2a_3 - 4f_Xa_2 + 4fa_3)}{8(f + Xa_2)^2}, \end{aligned} \quad (5)$$

where the subscripts ϕ and X denote the derivatives with respect to them. Since the DHOST theory contains the higher-order derivatives, it is useful to introduce the following quantity as the variation of the Lagrangian in the gravity sector with a variable A:

$$\mathcal{E}_A \coloneqq \frac{1}{\sqrt{-g}}\sum_{j=0}(-1)^j\partial_{\mu_1}\cdots\partial_{\mu_j}\frac{\delta(\sqrt{-g}\mathcal{L}_{\rm DHOST})}{\delta\partial_{\mu_1}\cdots\partial_{\mu_j}A}. \quad (6)$$

B. Background equations

We assume that the background metric is a flat Friedmann-Lemaître-Robertson-Walker metric (FLRW),

$$ds^2 = -N^2 dt^2 + a^2 \delta_{ij} dx^i dx^j. \tag{7}$$

By the use of the quantity defined in Eq. (6), one can easily write the background equation-of-motion for the lapse, the scale factor, and the scalar field. The explicit expressions for $\mathcal{E}_N, \mathcal{E}_a, \mathcal{E}_\phi$ are shown in Appendix A. With this, the governing equation of the scalar field is simply written as

$$\mathcal{E}_\phi = 0. \tag{8}$$

To get the evolution equation in the gravity sector, we have to take into account the matter content. We assume that the matter content is described as fluids. Hence, the energy-momentum tensor is given as

$$T^{\mu\nu} = \frac{2}{\sqrt{-g}} \frac{\delta\sqrt{-g}\mathcal{L}_m}{\delta g_{\mu\nu}} = \sum_{I=B,C,\gamma,\nu} (\rho_I + p_I) u_I^\mu u_I^\nu + p_I g^{\mu\nu}, \tag{9}$$

where ρ_I and p_I are the energy density and pressure of $I = b$ (baryon), c (CDM), γ (photon), ν (massless neutrinos), and u_I^μ is the 4-velocity of I, $u_I^\mu \coloneqq (u_I^0, v_I^i/a)$ with the velocity perturbation v_I^i. The zeroth order of the energy-momentum tensor is calculated as

$$T^{00} = \rho_{\rm s} \coloneqq \sum_I \rho_I, \qquad T^{ij} = \frac{\delta_{ij}}{a^2} p_{\rm s}, \qquad p_{\rm s} \coloneqq \sum_I p_I, \tag{10}$$

which satisfy the conservation law, $\dot{\rho}_s + 3H(\rho_s + p_s) = 0$, where a dot denotes the derivative with respect to t. Because the variations with respect to N and a can be rewritten in terms of those with respect to metric, $\delta/\delta N = -2\delta/\delta g_{00}$ and $\delta/\delta a = 2a\delta_{ij}(\delta/\delta g_{ij})$, we obtain the extended Friedmann equation and acceleration equation in the DHOST theory,

$$\mathcal{E}_N = \rho_{\rm s}, \qquad -\frac{a}{3}\mathcal{E}_a = p_{\rm s}, \tag{11}$$

where the left-hand sides are defined in Eqs. (A1) and (A2).

C. Euler-Lagrange equations for perturbations

In this subsection, we briefly discuss the Euler-Lagrange equation derived from the full DHOST Lagrangian Eq. (3). Focusing on the scalar perturbations, we consider the metric perturbations in the Newton-gauge form, which is defined as

$$ds^2 = -(1+2\Psi)dt^2 + 2a^2 \partial_i \xi dt dx^i + a^2\left[(1+2\Phi)\delta_{ij} + \left(\partial_i\partial_i - \frac{1}{3}\delta_{ij}\triangle\right)\eta\right] dx^i dx^j \tag{12}$$

and the perturbation of the scalar field as

$$\phi(t, \boldsymbol{x}) = \phi_0(t) + \delta\phi(t, \boldsymbol{x}). \tag{13}$$

The Euler-Lagrange equation (6) for the perturbed variables, $\{\Psi, \Phi, \xi, \eta, \delta\phi\}$, can be derived by expanding the full action Eq. (3) up to the second order and varying the second-order action with respect to each variable. Although we do not show the explicit expression for each $\mathcal{E}_A$, we use the resultant Euler-Lagrange equations to determine the relation between the DHOST functions, $\{P(\phi, X), Q(\phi, X), f_2(\phi, X), a_i(\phi, X)\}$ and the EFT parameters, $\{\alpha_i(t), \beta_i(t)\}$ to be introduced in the later section.

III. LINEAR PERTURBATIONS IN EFFECTIVE DESCRIPTION OF DHOST

In this section, we reformulate the linear perturbations of gravity and matter in the DHOST theory, following the approach called the effective field theory of dark energy [24–32].

A. Effective quadratic action and EFT parameters

In the context of the EFT, the metric is usually written in the ADM form,

$$ds^2 = -N^2 dt^2 + h_{ij}(dx^i + N^i dt)(dx^j + N^j dt). \tag{14}$$

To study the linear perturbations for gravity and matter, we need to expand the action up to the second order around the flat FLRW background given in Eq. (7) with the gauge $N = 1$. In the unitary gauge, the perturbed variables are the lapse $\delta N \equiv N - 1$, the extrinsic curvature $\delta K_{ij} = K_{ij} - H h_{ij}$ and the three-dimensional Ricci curvature ${}^{(3)}R_{ij}$. To describe the effective action for the DHOST in the EFT language, we need to introduce the time and space derivatives of δN in the effective Lagrangian. The effective quadratic action in gravity sector is given as [24]

$$S^{(2)} = \int d^4x \sqrt{-g}\mathcal{L}^{(2)}, \tag{15}$$

with

$$\begin{aligned}\mathcal{L}^{(2)} \coloneqq \frac{M^2}{2}\bigg\{&\delta K_{ij}\delta K^{ij} - \left(1+\frac{2}{3}\alpha_L\right)\delta K^2 \\ &+ (1+\alpha_T)\left({}^{(3)}R\frac{\delta\sqrt{h}}{a^3} + \delta_2{}^{(3)}R\right) \\ &+ H^2\alpha_K\delta N^2 + 4H\alpha_B\delta K\delta N + (1+\alpha_H)R\delta N \\ &+ 4\beta_1\delta K\dot{\delta N} + \beta_2\dot{\delta N}^2 + \frac{\beta_3}{a^2}(\partial\delta N)^2\bigg\},\end{aligned} \tag{16}$$

where H is the Hubble parameter, M is the effective Planck mass, and δ_2 extracts the second-order terms of the metric perturbations. We have introduced the eight time-varying parameters characterizing the effective quadratic Lagrangian, labeled as $\{\alpha_L, \alpha_T, \alpha_K, \alpha_B, \alpha_H, \beta_1, \beta_2, \beta_3\}$. In addition to them, we introduce a parameter characterizing the time variation of the effective Planck mass,

$$\alpha_M = \frac{1}{HM^2}\frac{dM^2}{\partial t}. \tag{17}$$

With these nine EFT parameters, we can fully specify the linear perturbations in the DHOST class of gravity theories. In the unitary gauge, the scalar perturbations can be defined as

$$\begin{aligned}&\delta N = N-1, \qquad N^i = \delta^{ij}\partial_i\psi, \\ &h_{ij} = a^2 e^{2\zeta}\delta_{ij} + a^2\left(\partial_i\partial_i - \frac{1}{3}\delta_{ij}\triangle\right)\eta.\end{aligned} \tag{18}$$

It would be convenient to change the gauge to compare the results derived in the previous section where the scalar perturbation, $\delta\phi(t,\boldsymbol{x})$, is exposed. To recover the scalar degree of freedom, we perform the time-coordinate transformation $t \to t + \pi(t,\boldsymbol{x})$. In general, the infinitesimal coordinate transformation, $x^\mu \to \bar{x}^\mu = x^\mu + \epsilon^\mu$, for the metric perturbation $\delta g_{\mu\nu}$ is given as

$$\overline{\delta g}_{\mu\nu}(\bar{x}) = \delta g_{\mu\nu}(x) - \nabla_\mu\epsilon_\nu - \nabla_\nu\epsilon_\mu. \tag{19}$$

For the infinitesimal time translation, $t \to \bar{t} = t + \pi(t,\boldsymbol{x})$, the displacement vector is given as $\epsilon^\mu = (\pi, 0)$, and its dual vector is $\epsilon_\mu = g_{\mu\nu}\epsilon^\nu = (-\pi, 0)$, where we truncate the expansion at the first order of the perturbations. Hence, the gauge transformation implies the relation between Eqs. (12) and (18) as

$$\delta N = \Psi + \dot{\pi}, \qquad \zeta = \Phi + H\pi, \qquad \psi = \xi - \frac{1}{a^2}\pi, \tag{20}$$

where η leaves unchanged under the gauge transformation. Rewriting the quadratic Lagrangian (16) in terms of the new perturbative quantities, we have

$$\mathcal{L}^{(2)} = \mathcal{L}_0^{(2)} + \frac{1}{a^2}\mathcal{L}_2^{(2)} + \frac{1}{a^4}\mathcal{L}_4^{(2)}, \tag{21}$$

where $\mathcal{L}_i^{(2)}$ are shown in Appendix B.

As a result of the time-coordinate transformation, the homogeneous scalar field in the unitary gauge acquires the spatial dependence, $\phi(t) \to \phi_0(t) + \delta\phi(t,\boldsymbol{x})$. Thus, we can identify the spatial fluctuation as [34]

$$\pi \coloneqq -\frac{\delta\phi}{\dot{\phi}_0}. \tag{22}$$

B. Euler-Lagrange equations for perturbations with EFT parameters

Varying Eq. (21) with respect to Ψ, Φ, ξ, η, and π, we obtain the Euler-Lagrange equations for them in the Newton gauge. Respecting the relation Eq. (22), these Euler-Lagrange equations in the EFT can describe those derived from the original DHOST action *without* the degeneracy conditions in Eq. (5). Comparing the coefficients of these equations in the two difference approaches, one can easily find the correspondence between the EFT parameters, $\{\alpha_i(t), \beta_i(t)\}$, and the functions in the DHOST theory, $\{P(\phi,X), Q(\phi,X), f_2(\phi,X), a_i(\phi,X)\}$. We found the following relations:

$$M^2 = 2(f_2 + a_1\dot{\phi}_0^2), \tag{23}$$

$$M^2\beta_1 = \frac{1}{2}\dot{\phi}_0^2(-2a_2 - 4f_{2X} + a_3\dot{\phi}_0^2), \tag{24}$$

$$M^2\beta_2 = 2\dot{\phi}_0^2(a_1 + a_2 - (a_3+a_4)\dot{\phi}_0^2 + a_5\dot{\phi}_0^4), \tag{25}$$

$$M^2\beta_3 = 2\dot{\phi}_0^2(-2a_1 + 4f_{2X} + a_4\dot{\phi}_0^2), \tag{26}$$

$$M^2\alpha_L = -3(a_1+a_2)\dot{\phi}_0^2, \tag{27}$$

$$M^2\alpha_H = 2(2f_{2X} - a_1)\dot{\phi}_0^2, \tag{28}$$

$$HM^2\alpha_M = 2\dot{\phi}_0(f_{2\phi} + a_{1\phi}\dot{\phi}_0^2 + 2(a_1 - f_{2X} - a_{1X}\dot{\phi}_0^2)\ddot{\phi}_0), \tag{29}$$

$$M^2\alpha_T = -2a_1\dot{\phi}_0^2, \tag{30}$$

$$\begin{aligned}2HM^2\alpha_B = 2f_{2\phi}\dot{\phi}_0 &- 2H(2a_1 + 3a_2 - 2f_{2X})\dot{\phi}_0^2 \\ &- 2(2f_{2\phi X} + Q_X)\dot{\phi}_0^3 \\ &+ H(-3a_3 + 4a_{1X} + 12a_{2X})\dot{\phi}_0^4 \\ &+ (2(a_1 - 2a_2 - 6f_{2X})\dot{\phi}_0 \\ &+ (3a_3 - 2a_4 + 4a_{2X} + 8f_{2XX})\dot{\phi}_0^3 \\ &+ 2(a_5 - a_{3X})\dot{\phi}_0^5)\ddot{\phi}_0,\end{aligned} \tag{31}$$

and

$$
\begin{aligned}
M^2H^2\alpha_K = {} & 2(3H^2(a_1-4f_{2X}-3K_1(a_2+2f_{2X}))-P_X+Q_\phi)\dot{\phi}_0^2+6H(-3a_{2\phi}+2Q_X)\dot{\phi}_0^3 \\
& +(3H^2(9a_3-10a_{1X}-18a_{2X}+16f_{2XX}+K_1(5a_3+4a_{2X}+8f_{2XX}))+4P_{XX}-2Q_{\phi X})\dot{\phi}_0^4 \\
& +3H(4a_{2\phi X}+5a_{3\phi}-4Q_{XX})\dot{\phi}_0^5-6H^2(-2a_{1XX}-6a_{2XX}+(3+K_1)a_{3X})\dot{\phi}_0^6-6Ha_{3\phi X}\dot{\phi}_0^7 \\
& +4\dot{\phi}_0(-3(a_1+a_2)H-2(a_{1\phi}+a_{2\phi})\dot{\phi}_0+3H(2(a_3+a_4)+a_{1X}+a_{2X})\dot{\phi}_0^2 \\
& +(a_{1\phi X}+a_{2\phi X}+3(a_{3\phi}+a_{4\phi}))\dot{\phi}_0^3-3H(3a_5+a_{3X}+a_{4X})\dot{\phi}_0^4-(a_{3\phi X}+a_{4\phi X}+4a_{5\phi})\dot{\phi}_0^5 \\
& +3Ha_{5X}\dot{\phi}_0^6+a_{5\phi X}\dot{\phi}_0^7)\ddot{\phi}_0 \\
& +(4(a_1+a_2)+2(3(a_3+a_4)+5a_{1X}+5a_{2X})\dot{\phi}_0^2-2(12a_5+2a_{1XX}+2a_{2XX}+9a_{3X}+9a_{4X})\dot{\phi}_0^4 \\
& +(4a_{3XX}+4a_{4XX}+26a_{5X})\dot{\phi}_0^6-4a_{5XX}\dot{\phi}_0^8)\ddot{\phi}_0^2 \\
& +(-8(a_1+a_2)\dot{\phi}_0+4(3(a_3+a_4)+a_{1X}+a_{2X})\dot{\phi}_0^3-4(4a_5+a_{3X}+a_{4X})\dot{\phi}_0^5+4a_{5X}\dot{\phi}_0^7)\dddot{\phi}_0. \qquad (32)
\end{aligned}
$$

Here, all the functions are evaluated at the background values, that is, $\phi=\phi_0(t)$ and $X=-\dot{\phi}_0^2(t)$, and we defined the dimensionless time derivatives of the Hubble parameter,

$$
K_n := \frac{1}{H^{n+1}}\frac{d^nH}{dt^n}. \qquad (33)
$$

Before showing the Euler-Lagrange equations for the perturbed variables in terms of the EFT parameters, we should discuss the dependence on the background energy density ρ_s and pressure p_s, which are related to the background Euler-Lagrange quantities, $\mathcal{E}_N$ and $\mathcal{E}_a$, through Eq. (11). Even when the above relations, Eqs. (23)–(32), are taken into account, one finds that there are several residuals in the equations derived in the full DHOST Lagrangian (3), compared with those from Eq. (21). Following the EFT point of view, these residuals should be rewritten in terms of the background quantities. We actually confirm that all the residuals can be identified to be a function of ρ_s, p_s and their time derivatives, and the results of the full DHOST can be consistently reproduced.[1] The explicit expression of the Euler-Lagrange equations with the background term corrections is summarized in Appendix C.

Let us consider the type-I degeneracy condition in the context of the effective description of the DHOST theory. In the EFT language, the fully nonlinear type-I degeneracy condition Eq. (5) reduces to the simpler conditions for the EFT parameters as

$$
\alpha_L=0, \qquad \beta_2=-6\beta_1^2, \qquad \beta_3=-2\beta_1[2(1+\alpha_H)+\beta_1(1+\alpha_T)], \qquad (34)
$$

reducing the number of the free EFT parameters to six. With this reduced degeneracy conditions, the Euler-Lagrange equations for Ψ, Φ, ξ, η, and π in the Newton gauge are given as

$$
\begin{aligned}
-\frac{1}{M^2}\mathcal{E}_\Psi = {} & -6\beta_1^2\ddot{\Psi}-6H\beta_1\left((3+\alpha_M)\beta_1+\frac{2}{H}\dot{\beta}_1\right)\dot{\Psi}-\frac{2}{a^2}\beta_1(2+2\alpha_H+(1+\alpha_T)\beta_1)\triangle\Psi \\
& +H^2\left(6+12\alpha_B-\alpha_K-6(3+K_1+\alpha_M)\beta_1-\frac{6\dot{\beta}_1}{H}+\frac{2\rho_s}{H^2M^2}\right)\Psi+6\beta_1\ddot{\Phi} \\
& +6H\left(-(1+\alpha_B-(3+\alpha_M)\beta_1)+\frac{\dot{\beta}_1}{H}\right)\dot{\Phi}+\frac{2}{a^2}(1+\alpha_H)\triangle\Phi-6\beta_1^2\dddot{\pi}+6H\beta_1\left(1-(3+\alpha_M)\beta_1-\frac{2}{H}\dot{\beta}_1\right)\ddot{\pi} \\
& +H^2(6\alpha_B-\alpha_K+6K_1\beta_1)\dot{\pi}-\frac{2}{a^2}\beta_1(1+2\alpha_H+(1+\alpha_T)\beta_1)\triangle\dot{\pi}+\frac{2H}{a^2}\left(-\alpha_B+\alpha_H+\beta_1+\alpha_M\beta_1+\frac{\dot{\beta}_1}{H}\right)\triangle\pi \\
& +6H^3\left(-K_1(1+\alpha_B)+(K_2+K_1(3+\alpha_M))\beta_1+\frac{K_1}{H}\dot{\beta}_1+\frac{\dot{\rho}_s}{6H^3M^2}\right)\pi, \qquad (35)
\end{aligned}
$$

[1]We expect that the above equations including these missing terms can be consistently derived from the full EFT action taking into account the terms describing the background [27,28].

$$
\begin{aligned}
-\frac{1}{M^2}\mathcal{E}_\Phi = {}& 6\beta_1\ddot{\Psi}+6H\left(1+\alpha_B+(3+\alpha_M)\beta_1+\frac{\dot{\beta}_1}{H}\right)\dot{\Psi}+\frac{2}{a^2}(1+\alpha_H)\triangle\Psi \\
&+6H^2\left((1+\alpha_B)(3+K_1+\alpha_M)+\frac{\dot{\alpha}_B}{H}-\frac{p_s+\rho_s}{2H^2M^2}\right)\Psi-6\ddot{\Phi}-6H(3+\alpha_M)\dot{\Phi}+\frac{2}{a^2}(1+\alpha_T)\triangle\Phi \\
&-\frac{6p_s}{M^2}\Phi+6\beta_1\dddot{\pi}+6H\left(\alpha_B+(3+\alpha_M)\beta_1+\frac{\dot{\beta}_1}{H}\right)\ddot{\pi}+\frac{2}{a^2}\alpha_H\triangle\dot{\pi}+\frac{2}{a^2}H(-\alpha_M+\alpha_T)\triangle\pi \\
&+6H^2\left(K_1(-1+\alpha_B)+\alpha_B(3+\alpha_M)+\frac{\dot{\alpha}_B}{H}-\frac{p_s+\rho_s}{2H^2M^2}\right)\dot{\pi}-6H^3\left(K_2+K_1(3+\alpha_M)+\frac{\dot{p}_s}{2H^3M^2}\right)\pi,
\end{aligned}
\tag{36}
$$

$$
-\frac{1}{M^2}\mathcal{E}_\xi = 2\beta_1\triangle\dot{\Psi}+2H(1+\alpha_B)\triangle\Psi-2\triangle\dot{\Phi}+2\beta_1\triangle\ddot{\pi}+2H\alpha_B\triangle\dot{\pi}-2H^2\left(K_1+\frac{p_s+\rho_s}{2H^2M^2}\right)\triangle\pi,
\tag{37}
$$

$$
-\frac{1}{M^2}\mathcal{E}_\eta = -\frac{1}{3a^2}[(1+\alpha_H)\triangle\triangle\Psi+(1+\alpha_T)\triangle\triangle\Phi+\alpha_H\triangle\triangle\dot{\pi}-H(\alpha_M-\alpha_T)\triangle\triangle\pi],
\tag{38}
$$

and

$$
\begin{aligned}
-\frac{1}{M^2}\mathcal{E}_\pi = {}& 6\beta_1^2\dddot{\Psi}+6H\beta_1\left(1+2(3+\alpha_M)\beta_1+\frac{4\dot{\beta}_1}{H}\right)\ddot{\Psi}+6H^2\Bigg(-\alpha_B+\frac{1}{6}\alpha_K+\beta_1(6+K_1+2\alpha_M \\
&+(3+\alpha_M)(3+K_1+\alpha_M)\beta_1)+\frac{1}{H}(\beta_1^2\dot{\alpha}_M+2(1+2(3+\alpha_M)\beta_1)\dot{\beta}_1)+\frac{2}{H^2}(\dot{\beta}_1^2+\beta_1\ddot{\beta}_1)\Bigg)\dot{\Psi} \\
&+\frac{2}{a^2}\beta_1(1+2\alpha_H+(1+\alpha_T)\beta_1)\triangle\dot{\Psi}+\frac{2H}{a^2}\Bigg(-\alpha_B+\alpha_H+2(1+\alpha_H)(1+\alpha_M)\beta_1+(1+\alpha_M)(1+\alpha_T)\beta_1^2 \\
&+\frac{\beta_1}{H}(2\dot{\alpha}_H+\beta_1\dot{\alpha}_T)+\frac{2}{H}(1+\alpha_H+\beta_1+\alpha_T\beta_1)\dot{\beta}_1\Bigg)\triangle\Psi+H^3\Bigg(\frac{\dot{\rho}_s}{M^2H^3}+(\alpha_K-6\alpha_B)(3+\alpha_M) \\
&+6(K_2+(3+\alpha_M)^2)\beta_1+2K_1(-3-9\alpha_B+\alpha_K+9(3+\alpha_M)\beta_1) \\
&-\frac{6}{H}\dot{\alpha}_B+\frac{\dot{\alpha}_K}{H}+\frac{6}{H}\beta_1\dot{\alpha}_M+\frac{12}{H}(3+K_1+\alpha_M)\dot{\beta}_1+\frac{6}{H^2}\ddot{\beta}_1\Bigg)\Psi-6\beta_1\dddot{\Phi}+6H\left(\alpha_B-2(3+\alpha_M)\beta_1-\frac{2\dot{\beta}_1}{H}\right)\ddot{\Phi} \\
&+6H^2\left(\frac{p_s+\rho_s}{2H^2M^2}+K_1+3\alpha_B+K_1\alpha_B+\alpha_B\alpha_M-(3+\alpha_M)(3+K_1+\alpha_M)\beta_1+\frac{\dot{\alpha}_B}{H}-\frac{\beta_1\dot{\alpha}_M}{H}-\frac{2}{H}(3+\alpha_M)\dot{\beta}_1-\frac{\ddot{\beta}_1}{H^2}\right)\dot{\Phi} \\
&-\frac{2}{a^2}\alpha_H\triangle\dot{\Phi}-\frac{2H}{a^2}\left(\alpha_M+\alpha_H(1+\alpha_M)-\alpha_T+\frac{\dot{\alpha}_H}{H}\right)\triangle\Phi+6\beta_1^2\ddddot{\pi}+12\beta_1H\left((3+\alpha_M)\beta_1+\frac{2\dot{\beta}_1}{H}\right)\dddot{\pi} \\
&+H^2\left(\alpha_K+6\beta_1(-2K_1+(3+\alpha_M)(3+K_1+\alpha_M)\beta_1)+\frac{6\beta_1}{H}(\beta_1\dot{\alpha}_M+4(3+\alpha_M)\dot{\beta}_1)+\frac{12}{H^2}(\dot{\beta}_1^2+\beta_1\ddot{\beta}_1)\right)\ddot{\pi} \\
&+H^3\left(\alpha_K(3+2K_1+\alpha_M)-12(K_2+K_1(3+\alpha_M))\beta_1+\frac{\dot{\alpha}_K}{H}-\frac{12}{H}K_1\dot{\beta}_1\right)\dot{\pi} \\
&+\frac{2}{a^2}\beta_1(2\alpha_H+(1+\alpha_T)\beta_1)\triangle\ddot{\pi}+\frac{1}{a^2}\Bigg(2\beta_1(H(1+\alpha_M)(2\alpha_H+(1+\alpha_T)\beta_1)+2\dot{\alpha}_H+\beta_1\dot{\alpha}_T) \\
&+4(\alpha_H+(1+\alpha_T)\beta_1)\dot{\beta}_1\Bigg)\triangle\dot{\pi}+\frac{2H^2}{a^2}\Bigg(K_1+(1+K_1+\alpha_M)(\alpha_B-\alpha_H)-\alpha_M+\alpha_T \\
&-(1+\alpha_M)(1+K_1+\alpha_M)\beta_1+\frac{1}{H}(\dot{\alpha}_B-\dot{\alpha}_H-\beta_1\dot{\alpha}_M-2(1+\alpha_M)\dot{\beta}_1)-\frac{\ddot{\beta}_1}{H^2}+\frac{p_s+\rho_s}{2H^2M^2}\Bigg)\triangle\pi \\
&+6H^4(K_2\alpha_B-(K_3+2K_2(3+\alpha_M))\beta_1+K_1(3+\alpha_M)(\alpha_B-(3+\alpha_M)\beta_1)+K_1^2(1+\alpha_B-(3+\alpha_M)\beta_1) \\
&+\frac{1}{H}\left(K_1(\dot{\alpha}_B-\beta_1\dot{\alpha}_M)-2(K_2+K_1(3+\alpha_M))\dot{\beta}_1)-\frac{K_1}{H^2}\ddot{\beta}_1-\frac{\dot{p}_s+\dot{\rho}_s}{2H^3M^2}-\frac{\ddot{\rho}_s}{6H^4M^2}\right)\pi,
\end{aligned}
\tag{39}
$$

where ρ_s and p_s are evaluated through the background evolution equations Eq. (11). Plugging Eqs. (23)–(32) and Eq. (11) into Eqs. (35)–(39), one can straightforwardly reproduce the Euler-Lagrange equations derived from the full DHOST theory.

C. Perturbed matter energy-momentum tensor

The perturbations of the energy-momentum tensor given in Eq. (9) are calculated as

$$\delta T^{00} = \sum_I \rho_I(\delta_I - 2\Psi), \quad \delta T^{ij} = \frac{1}{a^2}\sum_I(\delta p_I - 2p_I\Phi)\delta^{ij},$$
$$T^{0i} = \frac{1}{a}\sum_I(\rho_I + p_I)v_I^i. \tag{40}$$

For the baryons and CDM, the pressure and its perturbation satisfy $p_{b,c} = \delta p_{b,c} = 0$, whereas those for the photons and neutrinos satisfy $p_{\gamma,\nu} = \rho_{\gamma,\nu}/3$ and $\delta p_{\gamma,\nu} = \delta\rho_{\gamma,\nu}/3$. Then, performing the Fourier transformation for Eqs. (35)–(38), we find

$$-\frac{1}{M^2}\mathcal{E}_\Psi = \mathcal{S}_\Psi \coloneqq -3H^2(\Omega_c\delta_c + \Omega_b\delta_b + \Omega_\gamma\delta_\gamma + \Omega_\nu\delta_\nu) + \frac{2\rho_s}{M^2}\Psi, \tag{41}$$

$$-\frac{1}{M^2}\mathcal{E}_\Phi = \mathcal{S}_\Phi \coloneqq 3H^2(\Omega_\gamma\delta_\gamma + \Omega_\nu\delta_\nu) - \frac{6p_s}{M^2}\Phi, \tag{42}$$

$$-\frac{1}{M^2}\mathcal{E}_\xi = \mathcal{S}_\xi \coloneqq kaH^2(3\Omega_c V_c + 3\Omega_b V_b + 4\Omega_\gamma V_\gamma + 4\Omega_\nu V_\nu), \tag{43}$$

$$-\frac{1}{M^2}\mathcal{E}_\eta = \mathcal{S}_\eta \coloneqq 4H^2k^2(\Omega_\gamma\Theta_{\gamma 2} + \Omega_\nu\Theta_{\nu 2}), \tag{44}$$

where $\Omega_I \coloneqq \rho_I/3M^2H^2$ and $\mathcal{E}_A$ are given in Eqs. (35)–(38). In the last equation, $\Theta_{\gamma\ell}$ and $\Theta_{\nu\ell}$ are the multipoles of the temperature fluctuations of photons and neutrinos, respectively, and in the first three equations, $\delta_\gamma = 4\Theta_{\gamma 0}$ and $V_\gamma = -3\Theta_{\gamma 1}$ where we define the velocity potential $V_I \coloneqq -ik_i v_I^i/k$.

As for the scalar field, the governing equation is given as

$$-\frac{1}{M^2}\mathcal{E}_\pi = 0 \tag{45}$$

with Eq. (39).

D. Reduction of higher-derivative equations

For later convenience, we define $\tilde{\mathcal{E}}_\xi \coloneqq k^{-2}\mathcal{E}_\xi/M^2$, $\tilde{\mathcal{E}}_\eta \coloneqq -k^{-4}\mathcal{E}_\eta/M^2$, and $\tilde{\mathcal{E}}_i \coloneqq -\mathcal{E}_i/M^2$ for other equations, and

$$\tilde{\mathcal{S}}_\xi \coloneqq -\frac{1}{k^2}\mathcal{S}_\xi = -a\frac{H^2}{k}(3\Omega_c V_c + 3\Omega_b V_b + 4\Omega_\gamma V_\gamma + 4\Omega_\nu V_\nu), \tag{46}$$

$$\tilde{\mathcal{S}}_\eta \coloneqq \frac{1}{k^4}\mathcal{S}_\eta = 4\frac{H^2}{k^2}(\Omega_\gamma\Theta_{\gamma 2} + \Omega_\nu\Theta_{\nu 2}) \tag{47}$$

in the Fourier space. Then the evolution equations become simpler form, $\tilde{\mathcal{E}}_A = \tilde{\mathcal{S}}_A$ for $A = \Psi, \Phi, \xi, \eta$, and $\tilde{\mathcal{E}}_\pi = 0$. This equation, however, contains time derivatives of Ψ, Φ, and π up to the fourth order as given in Eq. (39). As the kinetic matrix of the highest derivatives of Ψ, Φ, and π are degenerated, we can eliminate such higher-order derivative terms. To do so, we define

$$\tilde{\mathcal{E}}_G \coloneqq -\tilde{\mathcal{E}}_\pi + \beta_1\dot{\tilde{\mathcal{E}}}_\Phi + (H(-\alpha_B + (3+\alpha_M)\beta_1) + 2\dot{\beta}_1)\tilde{\mathcal{E}}_\Phi, \tag{48}$$

which reads

$$\begin{aligned}\tilde{\mathcal{E}}_G = {}& \frac{2}{a^2}(\alpha_H + (1+\alpha_T)\beta_1)(\triangle\dot{\Phi} - \beta_1\triangle\dot{\Psi} - \beta_1\triangle\ddot{\pi}) + \frac{6}{M^2}(Hp_s(\alpha_B - 3\beta_1) - \beta_1\dot{p}_s - 2p_s\dot{\beta}_1)\Phi \\ & + \frac{2H}{a^2}(-\alpha_B(1+\alpha_T) + \gamma_3)\triangle\Phi - \frac{2H}{a^2}(\alpha_B\alpha_H + \beta_1\gamma_3)\triangle\dot{\pi} - \frac{2H}{a^2}(\alpha_H(1+\alpha_B) + \beta_1(1+\gamma_3+\alpha_T))\triangle\Psi \\ & + 6H^3\left(-\gamma_1 + \gamma_2 + \frac{2\dot{\alpha}_B\dot{\beta}_1}{H^2} + \frac{\beta_1\ddot{\alpha}_B}{H^2} + \left(\alpha_B - 3\beta_1 - \frac{2\dot{\beta}_1}{H}\right)\frac{p_s+\rho_s}{2H^2M^2} - \beta_1\frac{2\dot{p}_s + \dot{\rho}_s}{2H^3M^2}\right)\dot{\pi} \\ & + 6H^3\left(K_1(1+\alpha_B) - \gamma_1 + \gamma_2 + \frac{\dot{\alpha}_B}{H} + \frac{1}{H^2}(2\dot{\alpha}_B\dot{\beta}_1 + \beta_1\ddot{\alpha}_B - \ddot{\beta}_1) - \beta_1\frac{\dot{p}_s + \dot{\rho}_s}{2H^3M^2} + \left(1 + \alpha_B - 3\beta_1 - \frac{2\dot{\beta}_1}{H}\right)\frac{\rho_s + p_s}{2H^2M^2}\right)\Psi \\ & - 6H^2\left(K_1(1+\alpha_B) + \frac{\dot{\alpha}_B}{H} - \frac{\ddot{\beta}_1}{H^2} + (1+2\beta_1)\frac{p_s}{2H^2M^2} + \frac{\rho_s}{2H^2M^2}\right)\dot{\Phi}\end{aligned}$$

$$+\frac{2H^2}{a^2}\left(\gamma_3-K_1(1-\alpha_H+\alpha_B-(1+\alpha_T)\beta_1)-\alpha_B(1+\alpha_T)-\frac{1}{H}\dot{\alpha}_B+\frac{\ddot{\beta}_1}{H^2}-\frac{p_s+\rho_s}{2H^2M^2}\right)\triangle\pi$$
$$-6H^2\left(\alpha_B^2+\frac{1}{6}\alpha_K-K_1\beta_1(1+2\alpha_B)-\alpha_B(3+\alpha_M)\beta_1-\frac{1}{H}(2\beta_1\dot{\alpha}_B+\alpha_B\dot{\beta}_1)+\frac{\beta_1\ddot{\beta}_1}{H^2}+\beta_1\frac{p_s+\rho_s}{2H^2M^2}\right)(\ddot{\pi}+\dot{\Psi})$$
$$-6H^4\left(K_1^2(1+\alpha_B)+\frac{K_1}{H}\dot{\alpha}_B-\frac{K_1}{H^2}\ddot{\beta}_1-\left(1+\alpha_B-3\beta_1-\frac{2\dot{\beta}_1}{H}\right)\frac{\dot{p}_s}{2H^3M^2}-\frac{\dot{\rho}_s}{2H^3M^2}-\frac{\ddot{p}_s-3\beta_1\ddot{p}_s}{6H^4M^2}\right)\pi, \tag{49}$$

where

$$\gamma_1 \coloneqq \left(\alpha_B^2+\frac{1}{6}\alpha_K\right)(3+\alpha_M)-\alpha_B(K_2+(3+\alpha_M)^2)\beta_1+\frac{K_1}{3}\left(\alpha_K+3\alpha_B(-1+\alpha_B-3(3+\alpha_M)\beta_1)\right), \tag{50}$$

$$\gamma_2 \coloneqq \frac{1}{H}\left[2(3+K_1+\alpha_M)\beta_1\dot{\alpha}_B-\frac{1}{6}\dot{\alpha}_K-\alpha_B(\dot{\alpha}_B-\beta_1\dot{\alpha}_M-2(3+K_1+\alpha_M)\dot{\beta}_1)\right], \tag{51}$$

$$\gamma_3 \coloneqq \alpha_M-\alpha_T+(1+\alpha_M)(\alpha_H+(1+\alpha_T)\beta_1)+\frac{1}{H}(\dot{\alpha}_H+\beta_1\dot{\alpha}_T+2(1+\alpha_T)\dot{\beta}_1). \tag{52}$$

This expression will be used after the Fourier transformation. The corresponding source term is given as $\tilde{\mathcal{S}}_G \coloneqq \beta_1\dot{\tilde{\mathcal{S}}}_\Phi+(H(-\alpha_B+(3+\alpha_M)\beta_1)+2\dot{\beta}_1)\tilde{\mathcal{S}}_\Phi$. The resultant field equations for Ψ, Φ, and π contain the time derivatives up to the second order for π and the first order for Ψ and Φ. We note that the highest order of the derivative depends on the gravity theory of interest.

E. Evolution equations to solve

In what follows, we explain how to solve the set of equations in the type-I DHOST theory. As the unknown variables in the gravity sector are Ψ, Φ, and π, we need three independent equations. In this study, we choose

$$\tilde{\mathcal{E}}_\eta(\Phi,\Psi,\dot{\pi},\pi)=\tilde{\mathcal{S}}_\eta(\Theta_{\rm r2}), \tag{53}$$

$$\tilde{\mathcal{E}}_\xi(\dot{\Phi},\dot{\Psi},\ddot{\pi},\Psi,\dot{\pi},\pi)=\tilde{\mathcal{S}}_\xi(V_I), \tag{54}$$

$$\tilde{\mathcal{E}}_G(\dot{\Phi},\dot{\Psi},\ddot{\pi},\Phi,\Psi,\dot{\pi},\pi)=\tilde{\mathcal{S}}_G(\Phi,\delta_I,V_I), \tag{55}$$

where the right-hand sides of the first two equations are defined in Eqs. (46) and (47), and we shortly write $\delta_I=\{\delta_b,\delta_c,\delta_\gamma,\delta_\nu\}$, $V_I=\{V_b,V_c,V_\gamma,V_\nu\}$, and $\Theta_{{\rm r}i}=\{\Theta_{\gamma i},\Theta_{\nu i}\}$. The first time derivative of Eq. (53) becomes

$$\dot{\tilde{\mathcal{E}}}_\eta(\dot{\Phi},\dot{\Psi},\ddot{\pi},\Phi,\Psi,\dot{\pi},\pi)=\dot{\tilde{\mathcal{S}}}_\eta(V_I,\Theta_{\rm r2},\Theta_{\rm r3}), \tag{56}$$

where we have used the Boltzmann equation for $\Theta_{\gamma 2}$ and $\Theta_{\nu 2}$. Since the coefficient matrix of $\dot{\Phi},\dot{\Psi}$, and $\ddot{\pi}$ in Eqs. (54)–(56) is invertible, we can solve these equations with respect to $\dot{\Phi}$, $\dot{\Psi}$, and $\ddot{\pi}$, and obtain

$$\dot{\Phi}=\mathcal{F}_\Phi(\Phi,\Psi,\dot{\pi},\pi;\delta_I,V_I,\Theta_{\rm r2},\Theta_{\rm r3}), \tag{57}$$

$$\dot{\Psi}=\mathcal{F}_\Psi(\Phi,\Psi,\dot{\pi},\pi;\delta_I,V_I,\Theta_{\rm r2},\Theta_{\rm r3}), \tag{58}$$

$$\ddot{\pi}=\mathcal{F}_\pi(\Phi,\Psi,\dot{\pi},\pi;\delta_I,V_I,\Theta_{\rm r2},\Theta_{\rm r3}). \tag{59}$$

These equations can be straightforwardly derived, though the right-hand sides of these equations are too long to show here. Once one solves this set of equations numerically, one can obtain the time evolution of Φ, Ψ, π. Unfortunately, however, it is failed since the equation for $\dot{\Psi}$ seems to be unstable at late time. The easiest way to avoid the numerical instability is to replace Eq. (58) by a constraint equation Eq. (53), and we compute Ψ from Eq. (53) after updating Φ and π by solving Eqs. (57) and (59).

IV. NUMERICAL SETUP

We developed a Boltzmann solver implementing the framework of the DHOST theory. Our numerical code CMB2ND[2] solves the Boltzmann equations for photons, $\Theta_{\gamma\ell}$, and massless neutrinos, $\Theta_{\nu\ell}$, the continuity equations and the Euler equations for baryons and CDM, δ_b, V_b, δ_c, V_c, the modified Einstein equations for Ψ, Φ in the conformal Newtonian gauge, and the field equation for π given in Eqs. (57) and (59) with Eq. (53). One can find the basic equations in the matter sector in a standard textbook, e.g., Ref. [37].

[2]This Boltzmann code is not public yet, but we have confirmed that the numerical results with it precisely agree with those from CAMB (https://camb.info/). See also Refs. [35,36] in which one of the authors of this paper used the same code.

Respecting the scaling of the EFT parameters in Eq. (1), we can totally neglect the scalar field and its influence on the metric perturbations in the early time. Hence, we can impose the same initial conditions for the perturbative quantities as those given in GR,

$$\Psi = -\frac{10}{4f_\nu + 15}\zeta, \qquad \Phi = -\frac{4f_\nu + 10}{4f_\nu + 15}\zeta,$$
$$\Theta_{\nu 2} = -\frac{1}{12f_\nu + 45}\frac{k^2}{\mathcal{H}^2}\zeta, \quad \pi = 0, \tag{60}$$

where ζ is the curvature perturbation generated during inflation and $f_\nu = \rho_\nu/(\rho_\gamma + \rho_\nu)$.

To follow the same setup as in Ref. [26], we assume the ΛCDM background as a demonstration and $\alpha_{B,0}, \alpha_{T,0} < 0$, $\beta_{1,0}, \alpha_{H,0}, \alpha_{M,0} > 0$, and $\alpha_{K,0} = 1$. The choices of signature of the EFT parameters and their values are restricted to a certain range arising from the avoidance of the superluminality, ghost instability, and gradient instability of the scalar perturbation [24] (see also [26] in the GLPV theory). To put constrains on these parameters from the real observations, we have to take care of the appropriate range. Our aim in the present study, however, is to demonstrate the impact of these parameters on the angular power spectra. Hence, we adopt the above weak assumptions on the EFT parameters.

At this stage, we can freely choose the present values of the EFT parameters, $\alpha_{i,0}$ for $i = K, B, T, M, H$ and $\beta_{1,0}$. However the time-dependent functions $\alpha_i(t)$ and $\beta_i(t)$ are primarily described by the arbitrary functions $\{P(\phi, X), Q(\phi, X), f_2(\phi, X), a_i(\phi, X)\}$ introduced in the original DHOST Lagrangian [see Eq. (3)], and thus the EFT parameters should be related with each other. As we shall explain later, we also demonstrate this situation by adopting a model proposed by Crisostomi and Koyama [33] (CK) in which there is a cosmological solution exhibiting the late-time self-acceleration regime. In this model, α_i for $i = K, B, M, H$ and β_1 are described by four constants c_2, c_3, c_4, β, while α_T is fixed to be 0.

V. RESULTS IN EFT FRAMEWORK

In Fig. 1, we show the angular power spectra of the CMB temperature anisotropies, C_ℓ^{TT} (left), E-mode C_ℓ^{EE} (middle), and the lensing potential $C_\ell^{\phi\phi}$ (right). The gray band indicates the cosmic variance. To magnify the changes from the ΛCDM case, we also show the power spectra divided by those in ΛCDM model in Fig. 2. From the top to bottom, we show the parameter dependence on $\beta_{1,0}$, $\alpha_{H,0}$, $\alpha_{M,0}$, $\alpha_{T,0}$, and $\alpha_{B,0}$. We vary $\alpha_{i,0}$ with the order of $\mathcal{O}(0.1)$ and $\beta_{1,0}$ with that of $\mathcal{O}(0.01)$. In the present parametrization, a small change of β_1 yields a significant effect on the power spectra.

We find that these parameters affect the angular power spectrum of the temperature anisotropies only on the large scales through the integrated Sachs-Wolfe (ISW) effect as expected. In contrast, as the scalar metric perturbations do not directly couple to the photon's E-mode polarization with $\ell = 2$, the changes of C_ℓ^{EE} are highly suppressed. In this sense, the information from the E-mode does not improve the constrains on the EFT parameters as far as we focus on the scalar metric perturbations. Taking a look at the power spectrum of the lensing potential provided in the top-right panel in Fig. 2 and the panel below this, the large influences from the two beyond-Horndeski parameters, α_H and β_1, appear on the different scales; nonzero α_H yields the significant deviation from ΛCDM at $\ell \sim 30$, while β_1 does at $\ell \sim 3$.

To understand the behavior of C_ℓ^{TT} and $C_\ell^{\phi\phi}$ with nonzero β_1 or α_H, we show the time evolution of the gravity potential, Ψ, in Fig. 3. The time derivative of the gravity potentials, $\dot{\Psi} - \dot{\Phi}$, sources the ISW effect. In the late time, as we can completely neglect the contribution of the anisotropic stress induced by the photons and massless neutrinos, $\Phi \approx -\Psi$ is achieved and therefore $\dot{\Psi} - \dot{\Phi} \approx 2\dot{\Psi}$ in this regime. Hence, the ISW effect on the CMB photons is characterized by $\dot{\Psi}$ as [37]

$$\Theta_\ell^{\mathrm{ISW}}(k, \eta_0) \approx 2\int_0^{\eta_0} \dot{\Psi}(k, \eta) j_\ell[k(\eta_0 - \eta)] d\eta, \tag{61}$$

where η_0 is the present conformal time and $j_\ell(x)$ is the spherical Bessel function. In the same time, the lensing potential, ϕ, is also determined by $\Psi - \Phi \approx 2\Psi$ in the integration with respect to time [38],

$$\phi_\ell(k, \eta_0) \approx -2\int_0^{\chi_{\mathrm{LSS}}} \frac{\chi_{\mathrm{LSS}} - \chi}{\chi_{\mathrm{LSS}}\chi} \Psi(k, \eta) \frac{j_\ell(k\chi)}{k\chi} d\chi, \tag{62}$$

where $\chi = \eta_0 - \eta$ is the comoving distance measured from the observer and χ_{LSS} is that to the last-scattering surface.

In the case with nonzero β_1 (upper panels), the gravity potential does not deviate from that in the ΛCDM case for $k = 0.001\ h\mathrm{Mpc}^{-1}$ (upper left), while it rapidly tends to be zero at the low redshift for $k = 0.01\ h\mathrm{Mpc}^{-1}$ (upper right). Hence, the time derivative, $|\dot{\Psi}|$, becomes larger than that in the ΛCDM case, which significantly enhances the angular power spectrum of the temperature anisotropy, C_ℓ^{TT}, through the ISW effect as shown in Fig. 2 (top-left panel). Regarding with the lensing potential which is determined by Ψ instead of $\dot{\Psi}$, the decay of the potential suppresses the lensing potential in the case with nonzero β_1 comparing with that in the ΛCDM case. This property can be observed in the top-right panel of Fig. 2.

On the other hand, in the case with nonzero α_H (lower panels in Fig. 3), one can find the almost same degree of the deviation from the ΛCDM case on both the large scale (lower left) and the intermediate scale (lower right). The distinctive feature in this case is that the deviation from the

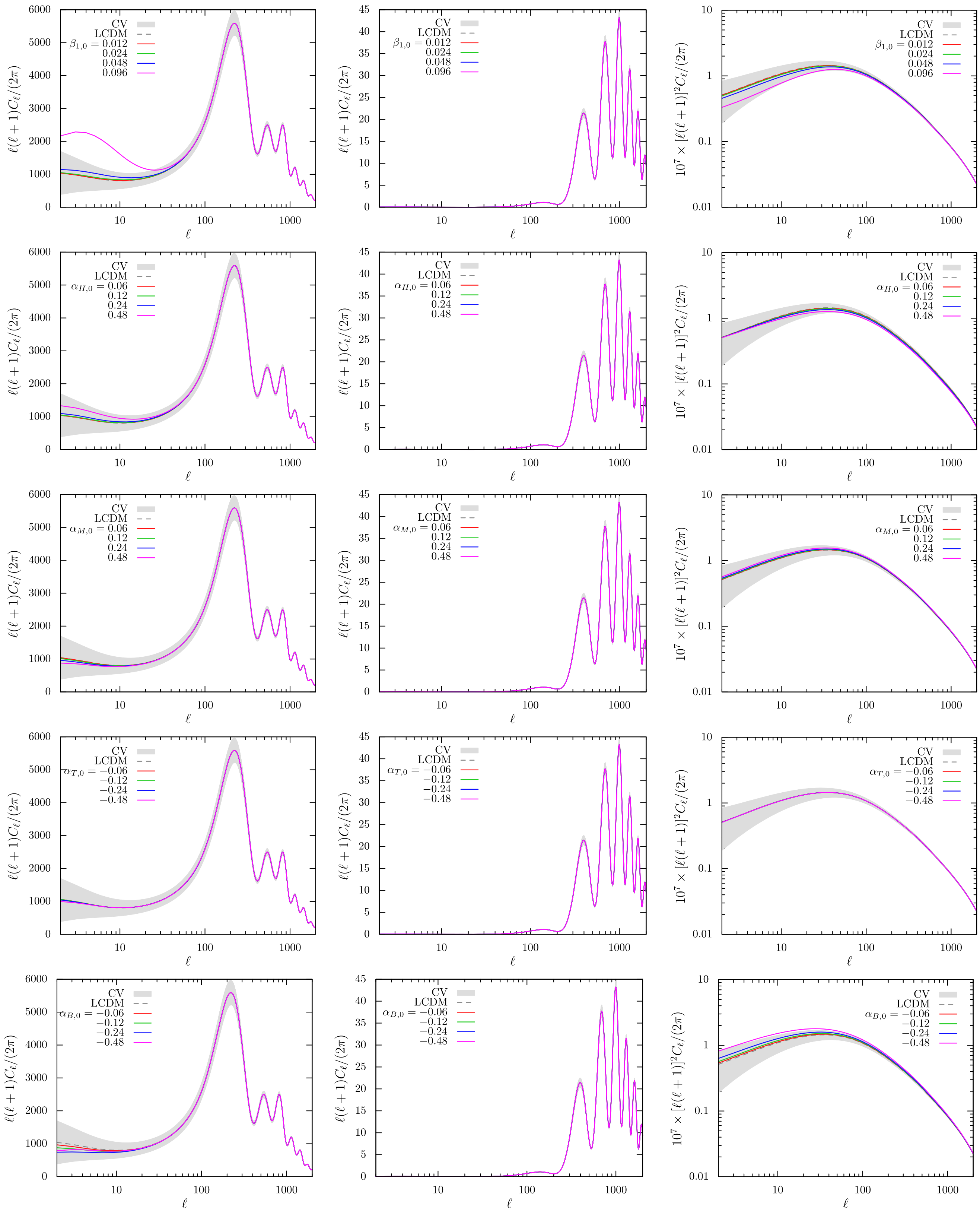

FIG. 1. Angular power spectra with varying $\beta_{1,0}$, $\alpha_{H,0}$, $\alpha_{M,0}$, $\alpha_{T,0}$, and $\alpha_{B,0}$ from top to bottom. From left to right, we show the angular power spectra of temperature (C_ℓ^{TT}), E-mode (C_ℓ^{EE}), and lensing potential ($C_\ell^{\phi\phi}$). The gray band indicates the cosmic variance (CV).

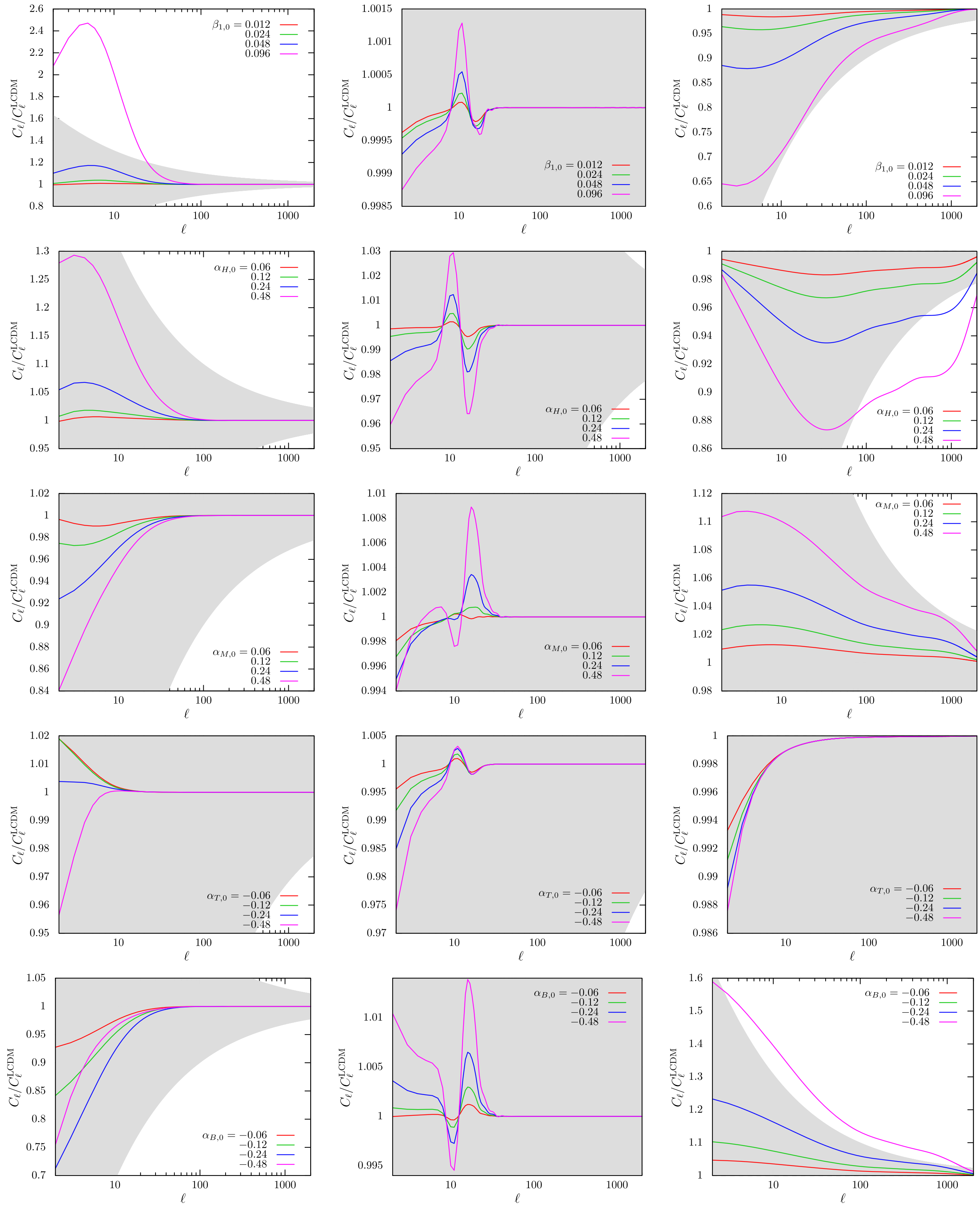

FIG. 2. The same power spectra in Fig. 1 divided by those in ΛCDM.

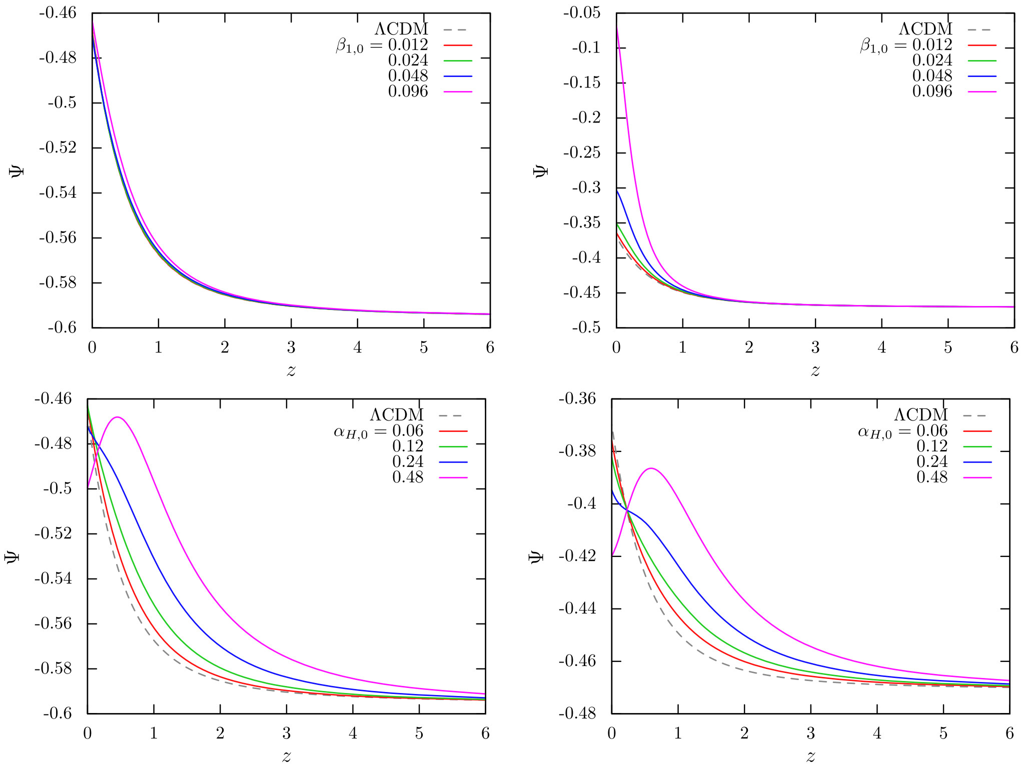

FIG. 3. The time evolution of Ψ with nonzero β_1 (upper) and with nonzero α_H (lower). In each case, we show the modes with $k = 0.001\ h\mathrm{Mpc}^{-1}$ (left) and $k = 0.01\ h\mathrm{Mpc}^{-1}$ (right).

ΛCDM case begins at relatively high redshift, $z \sim 5$, and the potential decays in the similar manner to the above case. However, at $z \lesssim 1$, the potential grows again, and its absolute value finally becomes larger than that in the ΛCDM case. It can be clearly seen for $\alpha_{H,0} = 0.24$, 0.48 (blue and magenta lines, respectively) at $z = 0$. The time derivative of the potential, $|\dot{\Psi}|$, is larger than that in the ΛCDM case over its whole life, enhancing C_ℓ^{TT} in the same manner of the previous case, though the enhancement is not so significant as shown in the second from top and left panels in Fig. 2. Regarding with $C_\ell^{\phi\phi}$, the decay of the gravity potential comparing with that in the ΛCDM case basically suppresses $C_\ell^{\phi\phi}$ in the whole range of ℓ in the second from top and right panels. However, the regrowth of the potential at the late time promotes the recovery of the lensing potential to the ΛCDM case on the angular large scale, say $\ell \lesssim 30$. For the smaller angular scales, this recovery property does not work, since the spherical Bessel function with a relatively large ℓ is exponentially suppressed for the small argument $k\chi$. As a result, there is a clear peak in the second from top and right panels in Fig. 2.

This fact indicates that, in principle, we can distinguish the effect from β_1 with that from α_H using the lensing potential, whereas it is difficult to do it only from the temperature anisotropies since the two effects on C_ℓ^{TT} are quite similar as shown in the left panels in Fig. 2. Note that the angular power spectra, C_ℓ^{TT} and $C_\ell^{\phi\phi}$, depending on $\alpha_{H,0}$ (the second panels from the top) and $\alpha_{B,0}$ (the bottom panels) in Figs. 1 and 2 reproduce the results in the pioneering work by D'Amico *et al.* [26] (and see also [39]).

To understand the suppression of $C_\ell^{\phi\phi}$ with $\beta_1 > 0$ on large scales in a different way, we define the following quantity [25,26]:

$$\mu_{\mathrm{WL}} \coloneqq \frac{2\nabla^2(\Psi - \Phi)}{3a^2H^2\Omega_m\delta_m}. \tag{63}$$

Here we focus on the case that matter is nonrelativistic: $\Omega_m\delta_m \approx \Omega_b\delta_b + \Omega_c\delta_c$ with $\Omega_m \approx \Omega_b + \Omega_c$ Since $\mu_{\mathrm{WL}} = 2$ for the case of the ΛCDM, $\mu_{\mathrm{WL}} - 2$ characterizes the deviation from the ΛCDM in weak lensing observations. To evaluate this quantity, we study the quasistatic evolution of the perturbations inside the sound horizon scale. Under such approximation, it is enough to consider the highest spatial derivative contributions in Eqs. (41), (42), and (45). Combining the governing equation of the density fluctuations, $\ddot{\delta}_M + 2H\dot{\delta}_M - \frac{1}{a^2}\nabla^2\Psi = 0$, we obtain μ_{WL} as a function of α_i and β_1 in addition to Ω_m.

If α_H is nonzero and the others set to be zero, we recover the result in Ref. [26],

$$\mu_{\mathrm{WL}} - 2 = \frac{\alpha_H(8 - 9\Omega_m(1 + \Omega_m))}{2 + 3\Omega_m(1 - \alpha_H)}, \tag{64}$$

where we have assumed $\dot{\delta}_m \approx H\delta_m$ for simplicity. When the denominator of the right-hand side is close to zero, the deviation from the ΛCDM, $\mu_{\rm WL} - 2$, can be very large. However, it is the case only if $\alpha_H \sim \mathcal{O}(1)$.

The situation drastically changes in the case with $\beta_1 \neq 0$. If β_1 is the only nonzero parameter, we obtain

$$\mu_{\rm WL} - 2 = \frac{6\beta_1[2(1-\Omega_m)(2+3\Omega_m(11-45\Omega_m)) - 9\beta_1\Omega_m^2(22+\Omega_m(19+3\Omega_m))]}{[-2+3\Omega_m(3+3\Omega_m(-3+\beta_1)+8\beta_1)][-2+9\Omega_m(1-3\Omega_m+(3+\Omega_m)\beta_1)]}. \tag{65}$$

In this case, $\mu_{\rm WL} - 2$ can be very large even if $\beta_1 \sim \mathcal{O}(0.1)$. That is why small β_1 has a large impact on $C_\ell^{\phi\phi}$ comparing with the other cases as shown in Fig. 2.

Next, we estimate the 1-sigma uncertainty in estimating the EFT parameters in the Fisher analysis. In the present study, we do not aim at putting constraints on the EFT parameters by assuming a realistic setup such as Planck or CMB-S4, but quantify the significance of the changes from the ΛCDM case. So we compute the Fisher matrix for each EFT parameter in the cosmic-variance-limited case with $f_{\rm sky} = 1$. Besides, we fix the other cosmological parameters according to the Planck 2015 data best fit, $h^2\Omega_{\rm CDM} = 0.120$, $h^2\Omega_{\rm b} = 0.0222$, $\tau = 0.078$, $h = 0.673$, $A_s = 2.14 \times 10^{-9}$ at $k = 0.05$ Mpc^{-1}, and $n_s = 0.967$ [40]. This treatment will certainly give the minimum values of the 1-sigma uncertainties. We here consider C_ℓ^{TT}, C_ℓ^{TE}, and C_ℓ^{EE}. The inclusion of $C_\ell^{\phi\phi}$ would possibly improve the forecast. However, we have to take care of the error arising from the reconstruction of the lensing potential. For simplicity, we here do not use $C_\ell^{\phi\phi}$ to estimate the 1-sigma uncertainties.

The Fisher matrix for an EFT parameter at the present time, $\theta = \alpha_{B,0}, \alpha_{T,0}, \alpha_{M,0}, \alpha_{H,0}, \beta_{1,0}$, is defined as

$$F = \sum_{XY}\sum_{\ell}^{\ell_{\rm max}} \frac{\partial C_\ell^X}{\partial\theta}(\mathcal{C}_\ell^{-1})^{XY}\frac{\partial C_\ell^Y}{\partial\theta}, \tag{66}$$

where $X, Y = TT, TE, EE$ and

$$\mathcal{C}_\ell = \frac{2}{2\ell+1}\begin{pmatrix} (C_\ell^{TT})^2 & C_\ell^{TE}C_\ell^{TT} & (C_\ell^{TE})^2 \\ C_\ell^{TE}C_\ell^{TT} & \mathcal{C}_\ell^{TE,TE} & C_\ell^{EE}C_\ell^{TE} \\ (C_\ell^{TE})^2 & C_\ell^{EE}C_\ell^{TE} & (C_\ell^{EE})^2 \end{pmatrix}, \tag{67}$$

with

$$\mathcal{C}_\ell^{ab,cd} \coloneqq \frac{1}{2}(C_\ell^{ab}C_\ell^{cd} + C_\ell^{ac}C_\ell^{bd}). \tag{68}$$

As the major change on the angular power spectra in Figs. 1 and 2 appears on the large scales, we fix $\ell_{\rm max} = 1000$. The 1-sigma uncertainty of each parameter is given by $\Delta\theta = F^{-1/2}$. The derivative $\partial C_\ell^X/\partial\theta$ is computed as

$$\left.\frac{\partial C_\ell^X}{\partial\theta}\right|_{\theta=0} \approx \frac{-C_\ell^X(2\delta\theta) + 4C_\ell^X(\delta\theta) - 3C_\ell^X(0)}{2\delta\theta}, \tag{69}$$

where the fiducial value in our study is $\theta = 0$. If the 1-sigma uncertainty of an EFT parameter, $\Delta\alpha_{i,0}$ or $\Delta\beta_{1,0}$, is small, the corresponding EFT parameter has strong impacts on the angular power spectra. In other words, even small $\alpha_{i,0}$ or $\beta_{1,0}$ results in the significant change of angular power spectra on the large scale from the ΛCDM case. In Table I, we show the 1-sigma uncertainties in estimating $\alpha_{i,0}$ for $i = B, T, M, H$ and $\beta_{1,0}$ with keeping $\alpha_{K,0} = 1$. Then we find that β_1 could be constrained stronger than α_H, and that, if $\beta_1 < \mathcal{O}(0.1)$, the deviation from the ΛCDM case is too small to be observed from the large-scale CMB observations.

As we mentioned before, we do not use $C_\ell^{\phi\phi}$. The estimation of $\Delta\alpha_{i,0}, \Delta\beta_{1,0}$ when we take into account $C_\ell^{\phi\phi}$ is beyond the scope of our present study, since it highly depends on how we reconstruct the lensing potential. Note that the values in the table scale as $\Delta\alpha_{i,0}, \Delta\beta_{1,0} \propto f_{\rm sky}^{-1/2}$. On the large scales, the noise source is dominated by the cosmic variance, and thus the instrumental noise depending on observatories is not important. Hence, one can roughly reproduce the 1-sigma uncertainties of the EFT parameters with, for example, the Planck observations ($f_{\rm sky} = 0.75$) [23] and CMB-S4 ($f_{\rm sky} = 0.4$) [41].

TABLE I. The 1-sigma uncertainties for the estimation of the EFT parameters, $\Delta\alpha_{i,0}$ and $\Delta\beta_{1,0}$, in the cosmic-variance-limited case with $f_{\rm sky} = 1$. The fiducial model is ΛCDM. The values in this table scale roughly as $\Delta\alpha_{i,0}, \Delta\beta_{1,0} \propto f_{\rm sky}^{-1/2}$.

Parameter	TT	TT + pol
β_1	0.17	0.13
α_H	0.92	0.56
α_M	0.66	0.47
α_T	0.73	0.29
α_B	0.15	0.12

VI. DEMONSTRATION IN A SPECIFIC MODEL IN DHOST THEORY

A. Background evolution and EFT parameters

Up to here, we treat the EFT parameters as free functions of time. In the DHOST theory, however, these parameters are described by the arbitrary functions $P(\phi, X)$, $Q(\phi, X)$, $f_2(\phi, X)$, and $a_i(\phi, X)$ for $i = 1, \ldots, 5$. They are thus

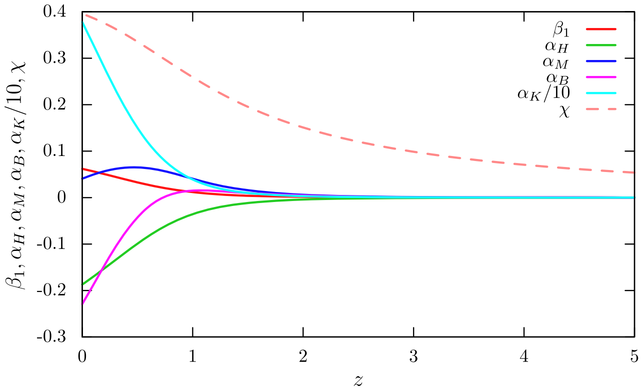

FIG. 4. Time evolution of β_1, α_i with $i = H, M, B, K$ (solid line) and $\chi(=\dot{\phi}_0)$ (dashed line) in the CK model with $(c_2, c_3, c_4, \beta) = (3.0, 5.0, 1.0, -5.3)$. As α_K is an order of magnitude larger than the others, we multiply it by $1/10$.

related with each other, and the cosmic expansion history also depends on these functions. We demonstrate the case in which the arbitrary functions are parametrized so that the resultant cosmic expansion is self-accelerated at late time. To do it, we adopt a parametrization proposed by Crisostomi and Koyama where the propagation speed of gravitational waves strictly coincides with the speed of light, $\alpha_T = 0$. [33].

To solve Eqs. (8) and (11), we fix the arbitrary functions, P, Q, f_2, and a_i. The condition, $\alpha_T = 0$, reads $a_1 = a_2 = 0$ from the first condition in Eqs. (5) and (30) [8]. Respecting this additional condition and the degeneracy condition given in Eq. (5), one finds that the remaining free functions are P, Q, f_2, and a_3. In Ref. [33], the authors propose the following parametrization:

$$P = c_2 X, \qquad Q = \frac{c_3}{\Lambda^3} X, \qquad f_2 = \frac{M_{\rm pl}^2}{2} + c_4 \frac{X^2}{\Lambda^6},$$
$$B_1 \coloneqq \frac{X}{4f_2}(4f_{2X} + a_3 X) = -\frac{X^2}{\frac{M_{\rm pl}^2}{2} + c_4 \frac{X^2}{\Lambda^6}} \frac{\beta}{4\Lambda^6}. \tag{70}$$

This model has the shift symmetry, $\phi \to \phi + \text{const.}$, and is parametrized by four constants, c_2, c_3, c_4, and β. The new energy scale Λ is given as $\Lambda = (M_{\rm pl} H^2)^{1/3}$.

Rescaling the time coordinate and the scalar field as $t \to M_{\rm pl}^{1/2} \Lambda^{-3/2} t$ and $\phi_0 \to M_{\rm pl} \phi_0$, we can reduce the equations (8) and (11) to those without any scales. The acceleration equation in Eq. (11) can be solved with respect to $\dot{H}$. Using this, we can eliminate $\dot{H}$ and $\ddot{H}$ in Eqs. (8) and (11). Eventually, these equations can be expressed in a simpler form as $U_1(\chi, a)\dot{\chi} + U_2(\chi, a) = 0, \dot{a}/a = U_3(\chi, a)$ where $\chi \coloneqq \dot{\phi}_0$. We do not explicitly show U_i, but they are given as functions of the cosmological parameters as well as the model parameters c_i, β. The initial value of χ is not sensitive to the final results since χ follows its attractor solution in the later time. After solving these equations, we can then rewrite the EFT parameters, $\alpha_i(t)$ and $\beta_1(t)$, in terms of $\chi(t)$, c_i, and β.

The time evolution of α_i, β_1, and χ are depicted in Fig. 4. As is shown in this figure, the EFT parameters become significant only at small z. In particular, in this model, $\beta_1 = (\beta/16c_4)\alpha_H$ is always satisfied. In the present case, β_1, α_H, and α_K are monotonically growing in time, while α_M and α_B are not. The nonmonotonic behavior of the EFT parameters has been pointed out in Ref. [42], where β_1 is "oscillated" at low z.

B. Angular power spectra

The angular power spectra, C_ℓ^{TT}, C_ℓ^{EE}, and $C_\ell^{\phi\phi}$, in the CK model with $(c_2, c_3, c_4, \beta) = (3.0, 5.0, 1.0, -5.3)$ are shown in Figs. 5 and 6. Although β_1 and α_H deviate from zero more than the range that we show in Fig. 1, C_ℓ^{TT} and C_ℓ^{EE} are not significantly deviated from those in ΛCDM on large scales. That is because these parameters are correlated so that the large negative α_H cancels the large positive β_1.

In contrast, one can observe the large deviation from ΛCDM on small scales. The choice of parameters, c_2, c_3, c_4, and β, in this demonstration recovers the cosmic expansion history in ΛCDM as reported in Ref. [33]. There is, however, a small change of expansion history

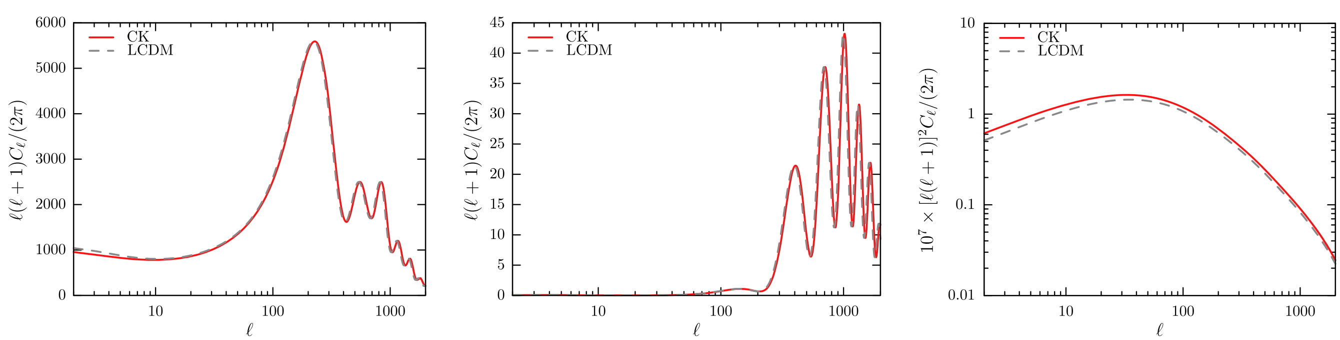

FIG. 5. Angular power spectra in CK model. From left to right, we show the angular power spectra of temperature (C_ℓ^{TT}), E-mode (C_ℓ^{EE}), and lensing potential ($C_\ell^{\phi\phi}$).

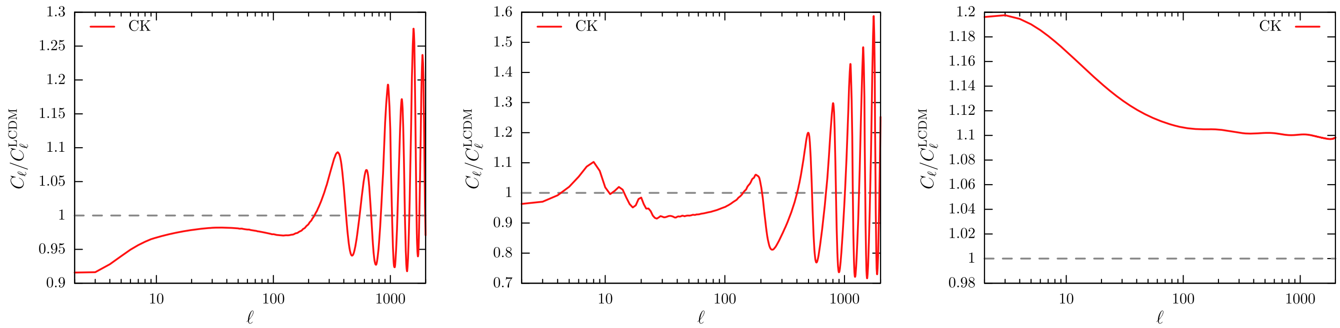

FIG. 6. The same power spectra in Fig. 5 divided by those in ΛCDM.

around the beginning of the dark energy epoch at $z \lesssim 1$. This fact induces a small change of the angular diameter distance of the horizon scale at the last scattering surface measured from us, and thus the peak location of the acoustic oscillations on small scales is a little bit shifted.

The small change of the angular diameter distance significantly affects $C_\ell^{\phi\phi}$ over the whole range of ℓ that can be observed in the present time. However, it does not immediately lead to the observability of these signals, since we cannot directly observe $C_\ell^{\phi\phi}$, but it is reconstructed from the combination of other observations such as the large-scale structure. We thus envisage that a large error induced from the reconstruction process makes it difficult to constrain the CK model only from $C_\ell^{\phi\phi}$. Our present study does not intend to mention how well we can constrain the CK model from these angular power spectra. Hence, we leave the detail analysis for the observability for future study.

VII. CONCLUSION

In the present study, we have investigated the impact of the deviation from GR on the angular power spectra of CMB anisotropies using the type-I DHOST theory. We first formulated the linear perturbations in the DHOST theory and their effective description parametrized by time-varying EFT parameters, resulting in the governing equation of the metric perturbation Φ in Eq. (57) and that of the scalar perturbation $\pi := -\delta\phi/\dot{\phi}_0$ in Eq. (59). Based on the effective description, we developed a Boltzmann solver implementing the DHOST theory. Solving the equations for the scalar perturbation, baryon, CDM, photon, massless neutrinos, and the metric perturbations in the conformal Newtonian gauge, we particularly focused on the impact of the EFT parameter characterizing the DHOST theory, β_1, on the angular power spectra.

We then obtain the angular power spectra of the CMB temperature anisotropies (C_ℓ^{TT}), E-mode polarization (C_ℓ^{EE}), and the lensing potential ($C_\ell^{\phi\phi}$) using the parametrization given in Eq. (1). In Figs. 1 and 2, we show these angular power spectra and those normalized by the spectra in ΛCDM model as our main results. In Eq. (65), we derived the deviation in weak lensing observations from the ΛCDM model, $\mu_{\rm WL} - 2$, when $\beta_1 \neq 0$ and the other EFT parameters are set to be zero. From this, we found that the deviation becomes significant even if β_1 is small. The top-right panel in Fig. 2 clarifies this fact from our numerical computation, and the large change of growth history of the metric perturbations gives a significant impact on the CMB temperature anisotropies as shown in the top-left panel in Fig. 2. On the other hand, the E-mode polarization is not so sensitive to this, since the polarization mode does not directly couple to gravity but is affected only through the quadrupole moment of the temperature anisotropy. To quantify the impact of the EFT parameters on the angular power spectra, we estimate the 1-sigma uncertainty in estimating them by computing the Fisher matrix assuming the ΛCDM model as the fiducial model. The results in the cosmic-variance-limited case are summarized in Table I. We found that, in principle, we can reach $\beta_1 \sim \mathcal{O}(0.1)$ from the large-scale CMB observations.

Finally, we demonstrate a specific model proposed by Ref. [33] which is a subclass of the DHOST theory with $\alpha_T = 0$. In our EFT approach, the background is fixed to be ΛCDM, while in this specific model all of the EFT parameters as well as the cosmic expansion history are consistently determined from the time evolution of the background scalar field $\phi_0(t)$. The resultant angular power spectra with $(c_2, c_3, c_4, \beta) = (3.0, 5.0, 1.0, -5.3)$, a parameter set proposed in Ref. [33] realizing the self-accelerating Universe, are shown in Figs. 5 and 6. As there are degeneracies among the EFT parameters, the parameters can vary in a larger range keeping the cosmic expansion history similar to that in ΛCDM model as shown in Fig. 4. This is not the case when only one of the parameters can be varied with $\alpha_{K,0} = 1$. In this specific model, we find the 8% suppression from ΛCDM in the temperature anisotropies on large scales, and $\mathcal{O}(10)\%$ deviation on small scales caused by the small change of the angular diameter distance to the last-scattering surface due to the tiny change of the cosmic expansion history around the transition to the dark energy domination epoch. As for the lensing potential, there are huge deviation from the ΛCDM model over the whole range of angular scales. However, this fact does not immediately conclude that it is easy to put a strong constraint on the deviation from ΛCDM, since the lensing potential should be reconstructed through a statistical process. In addition, it depends on how to parametrize the arbitrary functions in the DHOST theory to put constrains on the deviation from ΛCDM. Hence, we leave the quantitative study for the future.

ACKNOWLEDGMENTS

We would like to thank Tsutomu Kobayashi, Shinji Mukohyama, Kazuya Koyama, Atsushi Naruko, Kazufumi Takahashi, and Shin'ichi Hirano for giving fruitful comments and helpful discussion. This work was supported in part by MEXT/JSPS KAKENHI Grants No. JP17K14304 and JP19H01891 (D. Y.).

APPENDIX A: EULER-LAGRANGE EQUATIONS FOR THE BACKGROUND VARIABLES

The variations of the Lagrangian in the gravity sector defined in Eq. (6) with respect to N, a, and ϕ are computed as

$$\begin{aligned}\mathcal{E}_N \coloneqq{}& P+6f_2H^2+6Hf_{2\phi}\dot\phi_0+(-9a_1H^2+2P_X-Q_\phi+12f_{2X}(2H^2+\dot H)+a_2(-9H^2+6\dot H))\dot\phi_0^2\\ &+6H(a_{2\phi}-Q_X)\dot\phi_0^3+(6H^2(a_{1X}+3a_{2X})-3a_3(3H^2+\dot H))\dot\phi_0^4-3Ha_{3\phi}\dot\phi_0^5\\ &+(6H(a_1-2f_{2X})\dot\phi_0+2(a_{1\phi}+a_{2\phi})\dot\phi_0^2-3(a_3+2a_4)H\dot\phi_0^3-2(a_{3\phi}+a_{4\phi})\dot\phi_0^4+6a_5H\dot\phi_0^5+2a_{5\phi}\dot\phi_0^6)\ddot\phi_0\\ &+(-a_1-a_2+(-a_3-a_4-2(a_{1X}+a_{2X}))\dot\phi_0^2+(3a_5+2(a_{3X}+a_{4X}))\dot\phi_0^4-2a_{5X}\dot\phi_0^6)\ddot\phi_0^2\\ &+(2(a_1+a_2)\dot\phi_0-2(a_3+a_4)\dot\phi_0^3+2a_5\dot\phi_0^5)\dddot\phi_0,\end{aligned}\tag{A1}$$

$$\begin{aligned}-\frac{a}{3}\mathcal{E}_a \coloneqq{}& -P-2f_2(3H^2+2\dot H)-4Hf_{2\phi}\dot\phi_0+(-2f_{2\phi\phi}-Q_\phi+(a_1+3a_2)(3H^2+2\dot H))\dot\phi_0^2+2H(a_{1\phi}+3a_{2\phi})\dot\phi_0^3\\ &+(-2f_{2\phi}+4H(a_1+3a_2+2f_{2X})\dot\phi_0+2(a_{2\phi}+4f_{2\phi X}+Q_X)\dot\phi_0^2-4H(a_{1X}+3a_{2X})\dot\phi_0^3-a_{3\phi}\dot\phi_0^4)\ddot\phi_0\\ &+(-a_1+a_2+4f_{2X}+(-2a_3+a_4-4(a_{2X}+2f_{2XX}))\dot\phi_0^2+(-a_5+2a_{3X})\dot\phi_0^4)\ddot\phi_0^2\\ &+(2(a_2+2f_{2X})\dot\phi_0-a_3\dot\phi_0^3)\dddot\phi_0,\end{aligned}\tag{A2}$$

and

$$\begin{aligned}\mathcal{E}_\phi \coloneqq{}& P_\phi+6f_{2\phi}(2H^2+\dot H)+6(12H^3f_{2X}+HP_X-HQ_\phi+14Hf_{2X}\dot H-a_1(3H^3+2H\dot H)+2f_{2X}\ddot H+a_2(3H\dot H+\ddot H))\dot\phi_0\\ &+(2P_{\phi X}-3H^2(a_{1\phi}-9a_{2\phi}-8f_{2\phi X}+6Q_X)-Q_{\phi\phi}-6(-2(a_{2\phi}+f_{2\phi X})+Q_X)\dot H)\dot\phi_0^2\\ &+(6H(a_{2\phi\phi}-Q_{\phi X}+(a_{1X}+3a_{2X})(3H^2+2\dot H))-3a_3(9H(H^2+\dot H)+\ddot H))\dot\phi_0^3\\ &+(6H^2(a_{1\phi X}+3a_{2\phi X}-3a_{3\phi})-6a_{3\phi}\dot H)\dot\phi_0^4-3Ha_{3\phi\phi}\dot\phi_0^5+(2(P_X-Q_\phi+3a_1(2H^2+\dot H)+6f_{2X}(2H^2+\dot H)\\ &+a_2(9H^2+6\dot H))+6H(2a_{1\phi}+5a_{2\phi}-2Q_X)\dot\phi_0+(30H^2a_{1X}+2(a_{1\phi\phi}+a_{2\phi\phi}-2P_{XX}+Q_{\phi X})\\ &+6a_{2X}(9H^2-2\dot H)-24f_{2XX}(2H^2+\dot H)-3(5a_3+2a_4)(3H^2+\dot H))\dot\phi_0^2+3H(-9a_{3\phi}-4(a_{2\phi X}+a_{4\phi})+4Q_{XX})\dot\phi_0^3\\ &+(6H^2(-2a_{1XX}-6a_{2XX}+3a_{3X})-2(a_{3\phi\phi}+a_{4\phi\phi})+6a_{3X}\dot H+6a_5(3H^2+\dot H))\dot\phi_0^4\\ &+6H(a_{3\phi X}+2a_{5\phi})\dot\phi_0^5+2a_{5\phi\phi}\dot\phi_0^6)\ddot\phi_0+(3(a_{1\phi}+a_{2\phi})-18H(a_3+a_4+a_{1X}+a_{2X})\dot\phi_0-3(2(a_{1\phi X}+a_{2\phi X})\\ &+3a_{3\phi}+3a_{4\phi})\dot\phi_0^2+18H(2a_5+a_{3X}+a_{4X})\dot\phi_0^3+(6(a_{3\phi X}+a_{4\phi X})+15a_{5\phi})\dot\phi_0^4-18Ha_{5X}\dot\phi_0^5-6a_{5\phi X}\dot\phi^6)\ddot\phi_0^2\\ &+(-2(a_3+a_4+a_{1X}+a_{2X})+2(6a_5+2(a_{1XX}+a_{2XX})+5a_{3X}+5a_{4X})\dot\phi_0^2-2(2(a_{3XX}+a_{4XX})\\ &+9a_{5X})\dot\phi_0^4+4a_{5XX}\dot\phi_0^6)\ddot\phi_0^3+(12(a_1+a_2)H+4(a_{1\phi}+a_{2\phi})\dot\phi_0-12(a_3+a_4)H\dot\phi_0^2-4(a_{3\phi}+a_{4\phi})\dot\phi_0^3\\ &+12a_5H\dot\phi_0^4+4a_{5\phi}\dot\phi_0^5+(-8(a_3+a_4+a_{1X}+a_{2X})\dot\phi_0+8(2a_5+a_{3X}+a_{4X})\dot\phi_0^3-8a_{5X}\dot\phi_0^5)\ddot\phi)\dddot\phi_0\\ &+(2(a_1+a_2)-2(a_3+a_4)\dot\phi_0^2+2a_5\dot\phi_0^4)\ddddot\phi_0,\end{aligned}\tag{A3}$$

where we set $N=1$, and the subscripts ϕ and X stand for the derivative with respect to them. Here all the functions are evaluated at the background values, $\phi=\phi_0(t)$ and $X=-\dot\phi_0^2(t)$.

APPENDIX B: QUADRATIC LAGRANGIAN IN NEWTONIAN GAUGE

The quadratic Lagrangian defined in Eq. (21) after π is recovered by the coordinate transformation $t \to t + \pi(t, \boldsymbol{x})$ is given as

$$
\begin{aligned}
\frac{2}{M^2}\mathcal{L}_0^{(2)} = {} & -H^2(12\alpha_B - \alpha_K + 6(1+\alpha_L))\Psi^2 - 12H\beta_1\dot{\Psi}\Psi + 12H^2K_1\beta_1\dot{\Psi}\pi + 2H^2(-6\alpha_B + \alpha_K)\dot{\pi}\Psi \\
& + 12H^3K_1(1+\alpha_B+\alpha_L)\pi\Psi + H^2\alpha_K\dot{\pi}^2 + 12H(1+\alpha_B+\alpha_L)\dot{\Phi}\Psi + 12\beta_1\dot{\Phi}\,\dot{\Psi} + \beta_2\dot{\Psi}^2 - 12H\beta_1\ddot{\pi}\Psi \\
& + 2\beta_2\ddot{\pi}\,\dot{\Psi} - 6(1+\alpha_L)\dot{\Phi}^2 + 12H\alpha_B\dot{\Phi}\,\dot{\pi} - 12H^2K_1(1+\alpha_L)\dot{\Phi}\pi + 12\beta_1\dot{\Phi}\,\ddot{\pi} \\
& + 4\left(-H(1+\alpha_B+\alpha_L)\Psi - \beta_1\dot{\Psi} + (1+\alpha_L)\dot{\Phi} - \frac{\alpha_L}{6}\triangle\xi - H\alpha_B\dot{\pi} + H^2K_1(1+\alpha_L)\pi - \beta_1\ddot{\pi}\right)\triangle\xi \\
& + \frac{1}{6}(\triangle\dot{\eta})^2 - \frac{2}{3}\triangle\xi\triangle\dot{\eta} + 12H^3K_1\alpha_B\dot{\pi}\pi + \beta_2\ddot{\pi}^2 + 12H^2K_1\beta 1\ddot{\pi}\pi - 6H^4K_1^2(1+\alpha_L)\pi^2,
\end{aligned}
\tag{B1}
$$

$$
\begin{aligned}
\frac{2}{M^2}\mathcal{L}_2^{(2)} = {} & -\beta_3[\Psi\triangle\Psi + 2\Psi\triangle\dot{\pi} + \dot{\pi}\triangle\dot{\pi}] - 2[2(1+\alpha_H)\Psi + 2(1+\alpha_H)\dot{\pi} + (1+\alpha_T)\Phi + 2(1+\alpha_T)H\pi]\triangle\Phi \\
& + \frac{2}{3}\left((1+\alpha_T)\triangle\Phi + H(1+\alpha_T)\triangle\pi - \frac{1}{12}(1+\alpha_T)\triangle\triangle\eta + (1+\alpha_H)\triangle\Psi + (1+\alpha_H)\triangle\dot{\pi}\right)\triangle\eta \\
& + \left(4(-1+\alpha_B-\alpha_H)H\dot{\pi} - 4(1+\alpha_L)\dot{\Phi} + 4(\alpha_B - \alpha_H + \alpha_L)H\Psi\right. \\
& \left. -2(1+2K_1(1+\alpha_L)+\alpha_T)H^2\pi + 4\beta_1\ddot{\pi} + 4\beta_1\dot{\Psi} + \frac{4\alpha_L}{3}\triangle\xi + \frac{2}{3}\triangle\dot{\eta}\right)\triangle\pi,
\end{aligned}
\tag{B2}
$$

$$
\frac{2}{M^2}\mathcal{L}_4^{(2)} = -\frac{2}{3}\alpha_L(\triangle\pi)^2,
\tag{B3}
$$

where we integrate by part with respect to the spatial coordinates.

APPENDIX C: EULER-LAGRANGE EQUATIONS FOR METRIC AND SCALAR PERTURBATIONS

Varying the effective quadratic Lagrangian Eq. (16) with respect to Ψ, Φ, ξ, η, and π, and taking into account the terms describing the background, we obtain the Euler-Lagrange equations,

$$
\begin{aligned}
-\frac{1}{M^2}\mathcal{E}_\Psi = {} & \beta_2\dddot{\pi} + \beta_2\ddot{\Psi} + 6\beta_1\ddot{\Phi} + (H(6\beta_1 + (3+\alpha_M)\beta_2) + \dot{\beta}_2)\ddot{\pi} + (H(3+\alpha_M)\beta_2 + \dot{\beta}_2)\dot{\Psi} \\
& + 6(-H(1+\alpha_B+\alpha_L) + H(3+\alpha_M)\beta_1 + \dot{\beta}_1)\dot{\Phi} + H^2(6\alpha_B - \alpha_K + 6K_1\beta_1)\dot{\pi} \\
& + \left(H^2(6 + 12\alpha_B - \alpha_K + 6\alpha_L - 6(3+K_1+\alpha_M)\beta_1) + \frac{2\rho_s}{M^2} - 6H\dot{\beta}_1\right)\Psi + \frac{1}{a^2}(2\beta_1 + \beta_3)\triangle\dot{\pi} \\
& + \frac{1}{a^2}\beta_3\triangle\Psi + \frac{2}{a^2}(1+\alpha_H)\triangle\Phi + \frac{2}{a^2}(H(-\alpha_B + \alpha_H - \alpha_L + \beta_1 + \alpha_M\beta_1) + \dot{\beta}_1)\triangle\pi \\
& + \left(6H^2(H(-K_1(1+\alpha_B+\alpha_L) + (K_2 + K_1(3+\alpha_M))\beta_1) + K_1\dot{\beta}_1) + \frac{\dot{\rho}_s}{M^2}\right)\pi,
\end{aligned}
\tag{C1}
$$

$$
\begin{aligned}
-\frac{1}{M^2}\mathcal{E}_\Phi = {} & 6\beta_1\dddot{\pi} + 6\beta_1\ddot{\Psi} - 6(1+\alpha_L)\ddot{\Phi} + 6(H(\alpha_B + (3+\alpha_M)\beta_1) + \dot{\beta}_1)\ddot{\pi} + 6(H(1+\alpha_B+\alpha_L+(3+\alpha_M)\beta_1) + \dot{\beta}_1)\dot{\Psi} \\
& + (-6H(1+\alpha_L)(3+\alpha_M) - 6\dot{\alpha}_L)\dot{\Phi} + \left(6H(H(K_1(-1+\alpha_B-\alpha_L) + \alpha_B(3+\alpha_M)) + \dot{\alpha}_B) - \frac{3(p_s+\rho_s)}{M^2}\right)\dot{\pi} \\
& + \frac{2}{a^2}(\alpha_H - \alpha_L)\triangle\dot{\pi} + \frac{2}{a^2}(1+\alpha_H)\triangle\Psi + \frac{2}{a^2}(1+\alpha_T)\triangle\Phi - \frac{2}{a^2}(H(\alpha_M + \alpha_L(1+\alpha_M) - \alpha_T) + \dot{\alpha}_L)\triangle\pi \\
& + \left(6H(H(1+\alpha_B+\alpha_L)(3+K_1+\alpha_M) + \dot{\alpha}_B + \dot{\alpha}_L) - \frac{3(p_s+\rho_s)}{M^2}\right)\Psi - \frac{6p_s}{M^2}\Phi \\
& - 6H^3\left((1+\alpha_L)(K_2 + K_1(3+\alpha_M)) + \frac{1}{H}K_1\dot{\alpha}_L + \frac{\dot{p}_s}{2H^3M^2}\right)\pi,
\end{aligned}
\tag{C2}
$$

$$-\frac{1}{M^2}\mathcal{E}_\xi = 2\beta_1\triangle\ddot{\pi} + 2\beta_1\triangle\dot{\Psi} - 2(1+\alpha_L)\triangle\dot{\Phi} + 2H\alpha_B\triangle\dot{\pi} + 2H(1+\alpha_B+\alpha_L)\triangle\Psi - \frac{2}{3a^2}\alpha_L\triangle\triangle\pi + \left(-2H^2K_1(1+\alpha_L) - \frac{p_s+\rho_s}{M^2}\right)\triangle\pi, \tag{C3}$$

$$-\frac{1}{M^2}\mathcal{E}_\eta = -\frac{1}{3a^2}[\alpha_H\triangle\triangle\dot{\pi} + (1+\alpha_H)\triangle\triangle\Psi + (1+\alpha_T)\triangle\triangle\Phi - H(\alpha_M-\alpha_T)\triangle\triangle\pi], \tag{C4}$$

and the equation for π becomes

$$\begin{aligned}
-\frac{1}{M^2}\mathcal{E}_\pi = {}& -\beta_2\ddddot{\pi} - \beta_2\dddot{\Psi} - 6\beta_1\dddot{\Phi} - 2(H(3+\alpha_M)\beta_2 + \dot{\beta}_2)\dddot{\pi} + (6H\beta_1 - 2H(3+\alpha_M)\beta_2 - 2\dot{\beta}_2)\ddot{\Psi} \\
&+ (6H(\alpha_B - 2(3+\alpha_M)\beta_1) - 12\dot{\beta}_1)\ddot{\Phi} \\
&+ H^2\left(\alpha_K - 12K_1\beta_1 - (3+\alpha_M)(3+K_1+\alpha_M)\beta_2 - \frac{1}{H}\beta_2\dot{\alpha}_M - \frac{2}{H}(3+\alpha_M)\dot{\beta}_2 - \frac{\ddot{\beta}_2}{H^2}\right)\ddot{\pi} \\
&- H^2\Bigg(6\alpha_B - \alpha_K - 6(6+K_1+2\alpha_M)\beta_1 + (3+\alpha_M)(3+K_1+\alpha_M)\beta_2 \\
&+ \frac{1}{H}(\beta_2\dot{\alpha}_M - 12\dot{\beta}_1 + 2(3+\alpha_M)\dot{\beta}_2) + \frac{\ddot{\beta}_2}{H^2}\Bigg)\dot{\Psi} \\
&+ 6H^2\Bigg((3+\alpha_M)(\alpha_B - (3+\alpha_M)\beta_1) + K_1(1+\alpha_B+\alpha_L-(3+\alpha_M)\beta_1) \\
&+ \frac{1}{H}(\dot{\alpha}_B - \beta_1\dot{\alpha}_M - 2(3+\alpha_M)\dot{\beta}_1) - \frac{\ddot{\beta}_1}{H^2} + \frac{p_s+\rho_s}{2M^2H^2}\Bigg)\dot{\Phi} \\
&+ H^2(H(\alpha_K(3+2K_1+\alpha_M) - 12(K_2+K_1(3+\alpha_M))\beta_1) + \dot{\alpha}_K - 12K_1\dot{\beta}_1)\dot{\pi} + \frac{2\alpha_L}{3a^4}\triangle\triangle\pi \\
&- \frac{1}{a^2}(4\beta_1+\beta_3)\triangle\ddot{\pi} - \frac{1}{a^2}(2\beta_1+\beta_3)\triangle\dot{\Psi} - \frac{2}{a^2}(\alpha_H-\alpha_L)\triangle\dot{\Phi} - \frac{1}{a^2}(H(1+\alpha_M)(4\beta_1+\beta_3) + 4\dot{\beta}_1 + \dot{\beta}_3)\triangle\dot{\pi} \\
&- \frac{1}{a^2}(H(2(\alpha_B-\alpha_H+\alpha_L) + (1+\alpha_M)\beta_3) + \dot{\beta}_3)\triangle\Psi - \frac{2}{a^2}(H(\alpha_M + \alpha_H(1+\alpha_M) - \alpha_T) + \dot{\alpha}_H)\triangle\Phi \\
&+ \frac{2H^2}{a^2}\Bigg(K_1 + (1+K_1+\alpha_M)(\alpha_B-\alpha_H) + 2K_1\alpha_L - \alpha_M + \alpha_T - (1+\alpha_M)(1+K_1+\alpha_M)\beta_1 \\
&+ \frac{1}{H}(\dot{\alpha}_B - \dot{\alpha}_H - \beta_1\dot{\alpha}_M - 2(1+\alpha_M)\dot{\beta}_1) - \frac{\ddot{\beta}_1}{H^2} + \frac{p_s+\rho_s}{2M^2H^2}\Bigg)\triangle\pi \\
&+ H^3\Bigg((\alpha_K - 6\alpha_B)(3+\alpha_M) + 6(K_2 + (3+\alpha_M)^2)\beta_1 + 2K_1(-3 - 9\alpha_B + \alpha_K - 3\alpha_L + 9(3+\alpha_M)\beta_1) \\
&+ \frac{1}{H}(-6\dot{\alpha}_B + \dot{\alpha}_K + 6\beta_1\dot{\alpha}_M + 12(3+K_1+\alpha_M)\dot{\beta}_1) + \frac{6}{H^2}\ddot{\beta}_1 + \frac{\dot{\rho}_s}{M^2H^3}\Bigg)\Psi \\
&+ 6H^4\Bigg(K_2\alpha_B - (K_3 + 2K_2(3+\alpha_M))\beta_1 + K_1(3+\alpha_M)(\alpha_B - (3+\alpha_M)\beta_1) + K_1^2(1+\alpha_B+\alpha_L-(3+\alpha_M)\beta_1) \\
&+ \frac{1}{H}(K_1(\dot{\alpha}_B - \beta_1\dot{\alpha}_M) - 2(K_2 + K_1(3+\alpha_M))\dot{\beta}_1) - \frac{K_1}{H^2}\ddot{\beta}_1 - \frac{\dot{p}_s+\dot{\rho}_s}{2M^2H^3} - \frac{\ddot{\rho}_s}{6M^2H^4}\Bigg)\pi.
\end{aligned} \tag{C5}$$

[1] B. P. Abbott *et al.* (LIGO Scientific and Virgo Collaborations), Phys. Rev. Lett. **119**, 161101 (2017).
[2] B. P. Abbott *et al.* (LIGO Scientific and Virgo and Fermi-GBM and INTEGRAL Collaborations), Astrophys. J. **848**, L13 (2017).
[3] B. P. Abbott *et al.*, Astrophys. J. **848**, L12 (2017).
[4] J. M. Ezquiaga and M. Zumalacrregui, Phys. Rev. Lett. **119**, 251304 (2017).
[5] T. Baker, E. Bellini, P. Ferreira, M. Lagos, J. Noller, and I. Sawicki, Phys. Rev. Lett. **119**, 251301 (2017).
[6] J. Sakstein and B. Jain, Phys. Rev. Lett. **119**, 251303 (2017).
[7] P. Creminelli and F. Vernizzi, Phys. Rev. Lett. **119**, 251302 (2017).
[8] D. Langlois, R. Saito, D. Yamauchi, and K. Noui, Phys. Rev. D **97**, 061501 (2018).
[9] D. Langlois and K. Noui, J. Cosmol. Astropart. Phys. 02 (2016) 034.
[10] D. Langlois and K. Noui, J. Cosmol. Astropart. Phys. 07 (2016) 016.
[11] D. Langlois, Int. J. Mod. Phys. D **28**, 1942006 (2019).
[12] G. W. Horndeski, Int. J. Theor. Phys. **10**, 363 (1974).
[13] C. Deffayet, X. Gao, D. Steer, and G. Zahariade, Phys. Rev. D **84**, 064039 (2011).
[14] T. Kobayashi, M. Yamaguchi, and J. Yokoyama, Prog. Theor. Phys. **126**, 511 (2011).
[15] J. Gleyzes, D. Langlois, F. Piazza, and F. Vernizzi, Phys. Rev. Lett. **114**, 211101 (2015).
[16] J. Gleyzes, D. Langlois, F. Piazza, and F. Vernizzi, J. Cosmol. Astropart. Phys. 02 (2015) 018.
[17] T. Kobayashi, Y. Watanabe, and D. Yamauchi, Phys. Rev. D **91**, 064013 (2015).
[18] M. Crisostomi and K. Koyama, Phys. Rev. D **97**, 021301 (2018).
[19] A. Dima and F. Vernizzi, Phys. Rev. D **97**, 101302 (2018).
[20] S. Hirano, T. Kobayashi, and D. Yamauchi, Phys. Rev. D **99**, 104073 (2019).
[21] P. Creminelli, M. Lewandowski, G. Tambalo, and F. Vernizzi, J. Cosmol. Astropart. Phys. 12 (2018) 025.
[22] P. Creminelli, G. Tambalo, F. Vernizzi, and V. Yingcharoenrat, J. Cosmol. Astropart. Phys. 05 (2020) 002.
[23] N. Aghanim *et al.* (Planck Collaboration), Astron. Astrophys. **641**, A6 (2020).
[24] D. Langlois, M. Mancarella, K. Noui, and F. Vernizzi, J. Cosmol. Astropart. Phys. 05 (2017) 033.
[25] J. Gleyzes, D. Langlois, M. Mancarella, and F. Vernizzi, J. Cosmol. Astropart. Phys. 08 (2015) 054.
[26] G. D'Amico, Z. Huang, M. Mancarella, and F. Vernizzi, J. Cosmol. Astropart. Phys. 02 (2017) 014.
[27] J. K. Bloomfield, É. É. Flanagan, M. Park, and S. Watson, J. Cosmol. Astropart. Phys. 08 (2013) 010.
[28] G. Gubitosi, F. Piazza, and F. Vernizzi, J. Cosmol. Astropart. Phys. 02 (2013) 032; 02 (2013) 032.
[29] J. Gleyzes, D. Langlois, F. Piazza, and F. Vernizzi, J. Cosmol. Astropart. Phys. 08 (2013) 025.
[30] J. Bloomfield, J. Cosmol. Astropart. Phys. 12 (2013) 044.
[31] F. Piazza and F. Vernizzi, Classical Quantum Gravity **30**, 214007 (2013).
[32] J. Gleyzes, D. Langlois, and F. Vernizzi, Int. J. Mod. Phys. D **23**, 1443010 (2015).
[33] M. Crisostomi and K. Koyama, Phys. Rev. D **97**, 084004 (2018).
[34] E. Bellini and I. Sawicki, J. Cosmol. Astropart. Phys. 07 (2014) 050.
[35] T. Hiramatsu, E. Komatsu, M. Hazumi, and M. Sasaki, Phys. Rev. D **97**, 123511 (2018).
[36] T. Hiramatsu, S. Yokoyama, T. Fujita, and I. Obata, Phys. Rev. D **98**, 083522 (2018).
[37] S. Dodelson, *Modern Cosmology* (Academic Press, Amsterdam, 2003).
[38] D. Yamauchi, T. Namikawa, and A. Taruya, J. Cosmol. Astropart. Phys. 08 (2013) 051.
[39] D. Traykova, E. Bellini, and P. G. Ferreira, J. Cosmol. Astropart. Phys. 08 (2019) 035.
[40] P. A. R. Ade *et al.* (Planck Collaboration), Astron. Astrophys. **594**, A13 (2016).
[41] K. N. Abazajian *et al.* (CMB-S4 Collaboration), arXiv:1610.02743.
[42] S. Arai, P. Karmakar, and A. Nishizawa, Phys. Rev. D **102**, 024003 (2020).